CR 60002

Final Report

INVESTIGATIVE STUDY ALONG WITH DESIGN AND DEVELOPMENT OF AN ULTRAVIOLET AIR DENSITY METER

FR 63-427-2184

Contracts NAS 5-427 and NAS 5-2121

For

GODDARD SPACE FLIGHT CENTER

National Aeronautics and Space Administration

Washington 25, D. C

By

Delbert G. Van Ornam

19 December 1963

PLASMADYNE CORPORATION SANTA ANA CALIFORNIA

Final Report

INVESTIGATIVE STUDY ALONG WITH DESIGN AND DEVELOPMENT OF AN ULTRAVIOLET AIR DENSITY METER

FR123-427-2184

Contracts NAS 5-427 and NAS 5-2184

For

GODDARD SPACE FLIGHT CENTER

National Aeronautics and Space Administration
Washington 25, D. C.

By

Delbert G. Van Ornum

19 December 1963

PLASMADYNE CORPORATION, SANTA ANA, CALIFORNIA

ABSTRACT

2918 ϕ

This report describes the design, fabrication, and testing of an air density meter based on the measurement of the backscatter of ultraviolet light. It was determined that intermediate ultraviolet near .2 microns was particularly useful for measurements of this kind. It was shown that ambient atmospheric density measurements can be made at a position 2 meters removed from the detection instruments during daylight and avoiding aerodynamic disturbances caused by shock waves, boundary layers, ionization, outgassing, gage aperture velocity vector and gage chamber temperature. Ultimate use of the backscatter meter is expected to be able to be extended from the tropopause (11 km) to 100 km or over a molecular number density range of 7.6×10^{18} cm^{-3} to 7.7×10^{12} cm^{-3} as given by the 1959 ARDC Model Atmosphere (1). A flight test of the instrument was accomplished to an altitude of approximately 10 km.

Auth.

TABLE OF CONTENTS

LIST OF ILLUSTRATIONS

1.0 INTRODUCTION

The measurement of air density from a high speed vehicle at altitudes above the tropopause and to 100 km altitude is becoming increasingly important now that manned aircraft or spacecraft will be operating through this region. Meteors produce light while falling from 100 to 50 km and offer vivid proof of the critical thermal problem to be met in traversing these altitudes. The adaptation of pressure or density measuring techniques successful at low altitude and at low Mach numbers to high altitude and high Mach numbers is greatly complicated by the interaction between the vehicle and the atmosphere. Apertures and ducts leading to internal metering chambers introduce errors which vary with the attitude of the vehicle in the air stream. The ultraviolet backscatter technique offers a means of sampling air density at a distance away from the vehicle which is sufficient to avoid the aerodynamic disturbances caused by shock waves, boundary layers, outgassing, ionization, and other aerodynamic effects, all of which are shape and orientation dependent.

The backscatter of light has been used to measure air density in the stratosphere from ground based searchlight projectors in a number of experiments. Hulburt (2) in 1937 succeeded in photographing a searchlight beam to 28 km, and in 1955, Friedland, Katzenstein, Sherman and Zatzick (3) used a 20 microsecond 50 megalumen light pulse system to determine densities to an altitude of 40 km. Many of the problems inherent in such experiments are lacking if the light projector and the receiver are mounted on a vehicle moving through the atmosphere. The purpose of this project was to develop an air density meter which could be carried as a flight

instrument by a missile or manned vehicle.

The success of previous searchlight experiments offered considerable encouragement to the present project, first, because useful backscatter energy was obtained in spite of very large distances and secondly there was evidence that the scatter from altitudes above the tropopause was related to the molecular density and not appreciably distorted by particulate or Mie scattering. In other words, above the tropopause a predominantly Rayleigh atmosphere exists.

A first look at scatter theory shows that electromagnetic radiations in the visible and ultraviolet have much larger wavelengths than the radius of the air molecules so that backscatter efficiency increases rapidly as wavelength decreases. However, atmospheric absorption of the probing radiation becomes increasingly important in the ultraviolet. Sources of radiation also become more complex and optical systems more difficult to design at the very short wavelengths.

The following relation expresses the backscatter intensity, I, from a unit volume, at a distance, r, as a function of incident illumination in watts per cm^2, I_0, and the reflectivity of the atmosphere, η.

$$I_{(180^\circ)} = I_0 \, \eta \, r^{-2} \qquad (1)$$

The reflectivity term , η. is a function of light wavelength and the molecular number density. This means that in an instrument designed to use a particular wavelength and with a known I_o measuring the reflectivity or $I_{(180°)}$ directly measures the number density as well. To form some idea as to the feasibility of using such a technique at high altitude the following table has been computed, where r is the distance to and d is the depth of the scatter volume.

TABLE 1 -- Backscatter at .2 Microns

Altitude Kilometers	Reflectivity cm^{-1}	$I_{(180°)}$ per watt cm^{-2} (r = 10 cm, d = 1 cm)	(r = 10 m, d = 1 m)
11	4×10^{-7}	4×10^{-9}	4×10^{-11}
100	8×10^{-13}	8×10^{-15}	8×10^{-17}

If we assume the radiation detector used can respond to 10^{-12} watts, a value 100 times the noise equivalent power of a good photomultiplier tube, then we can estimate receiver areas and power of I_o required to obtain reflectivity data at high altitude. In the searchlight experiments very large receiving apertures were used along with light pulses of 10 to 100 kilowatts. For flight experiments one kilowatt in a fairly narrow band is possible but receiving apertures must of course be limited. An area of 100 cm^2 should be feasible, but an area of 1000 cm^2 is not realistic. The received scatter signal would then be:

TABLE 2 -- Backscatter Power at .2 Microns

Altitude Kilometers	$P_{(180°)}$ Watts for A = 100 cm^2 and $P_o = 10^3$ Watts (r = 10 cm, d = 1 cm)	(r = 10 m, d = 1 m)
11	4×10^{-4}	4×10^{-6}
100	8×10^{-10}	8×10^{-12}

It would then appear that if a transmitter beam power of 1 kilowatt per useful ultraviolet bandwidth can be achieved in vicinity of 0.2μ then backscatter measurements can be made to 100 kilometers altitude at distances as great as 10 meters from the vehicle. These estimates of course assume no background noise due to radiation from the atmosphere in the wavelengths used. A survey of existing continuous light sources indicates that obtaining 1 kilowatt in the intermediate ultraviolet would require quite a large unit, however, the use of pulsed or flash tube sources makes such powers feasible. The pulse must be long enough to return a relatively large number of photons to avoid in-signal noise due to statistical fluctuation in the number of electrons leaving the photocathode of the detecting photomultiplier.

Summarizing, we conclude that the Rayleigh backscatter technique of measuring atmospheric number density as demonstrated by searchlight experiments can be developed for use on high altitude vehicles.

2.0 SCATTER THEORY AND SOLAR BACKGROUND

The ultraviolet radiation scattered from the irradiated air volume under observation is always very small as compared to the total incident radiation of the beam. It is evident, however, that the detection of scattered solar radiation from sources other than the desired backscatter volume, results in noise and in impairment of the desired measurement. It is therefore important to reduce such interference by selecting the optimum wavelength band for the flight scatter experiments. The following paragraphs explore scatter theory and the likely solar radiation background.

2.1 Polarizability of Molecules

The ability of molecules to respond to the presence of an electric field is a measure of their polarizability. This response is in the nature of the formation of a particle electric moment. The magnitude of a particular moment is a function of the nature of the electronic distribution of the molecule.

Any particular electron of a molecule is influenced simultaneously by the Coulomb forces between it and all the other electrons and also between it and the positive cores of the atoms making up the molecule. The inter-electron forces are repulsive in action, and the electron-nuclear forces attractive. An individual electron is therefore pushed away by its electron neighbors and pulled in by the positive nuclear cores. These actions are taking place, of course, while the electron and its neighbors are moving around the nucleus with velocities which are at times comparable with the velocity of light. Accompanying the Coulomb forces, we know that there are other forces, so-called exchange or Pauli forces.

which act to prevent neighboring electrons from behaving similarly in a dynamical-way.

It is evident from the preceding considerations that when an electric field is impressed on a molecule, the ultimate electric moment acquired is the end result of a rather complicated competitive effort. Any theoretical evaluation requires the application of quantum mechanical methods to calculate realistic values. However, on the basis of such theoretical procedures, it is possible to formulate "rule of thumb" prescriptions which serve to provide fairly reliable values for the simpler molecules.

Calculation of the polarizability by quantum mechanical methods requires that the wave equation for the molecule with the interaction of the electric field on all the electrons and the nucleus included in the expression for the Hamiltonian be solved. In general this is not practicable in exact form. Recourse has to be had to approximate methods. The most common of these is the variational method. The latter is convenient when the molecule is originally in the ground state. The energy of the system will then be a minimum for the correct wave function of the system. Thus, one can use an approximate wave function with a number of adjustable parameters, varying the latter to minimize the energy, to get a good estimate of the proper electron distribution function. That part of the energy in the presence of an electrical field, which varies as the square of the electric field, serves to measure the degree of polarizability of the system.

Dimensionally, the expression for the polarizability behaves as the cube of a length. Following the procedures sketched in the preceding paragraphs, one finds that the polarizability for a simple atom will behave as the square of the average of the square of the radial distances of the electrons from the nucleus, and inversely, to a characteristic length of the atom, the Bohr radius, (0.53 Angstroms).

Expressions for the polarizability of molecules are somewhat more complicated, but the general structural relation is similar. An essential modification consists of a correlation term between pairs of electrons. In reality, such correlations cannot be evaluated without exact wave functions. However, fairly good approximations can be made from various combinations of atomic functions.

Where different electron groups act fairly independently of each other, the polarizability will obviously be made of the sum of the individual polarizabilities of the separate groups (bond polarizability sum rule).

An important result of such theoretical analyses is that one can see that in the formation of molecules, there can be serious deviations of the resultant polarizability from that which would come from the addition of the polarizabilities of the separate atoms. Thus, we find that the polarizability of the oxygen free radical is much less than the oxygen molecule. A density probe which relies on backscattering (Rayleigh scattering), from molecules and atoms, is thus also a composition probe. The backscattered signal detected depends not only on the

number of particles, but also the type.

By utilizing the frequency dependence of the polarizability, one can make the backscatter signal provide information both on the density and composition of the ambient gas. The number of independent observations must, of course, be equal to the number of independent composition variables. The actual polarizability data can be derived theoretically, and also from controlled experiments in the laboratory

The values of the polarizability of the constituents encountered in the atmosphere are given in the following summary. Included also, is the value for nitrous oxide.

TABLE 3 -- Polarizability at 589 mμ

Molecule	α
N_2	17.6×10^{-25} cm^3
O_2	16.0×10^{-25}
O	1.5×10^{-25}
N_2O	30.0×10^{-25}

As can be seen, the molecular form of nitrogen oxide does not yield a simple additive expression for the polarizability as a function of the separate polarizabilities of the individual atoms or radicals, nor does the polarizability of O_2 equal twice that of atomic oxygen.

The values given in the above table do not show the dependence on frequency. The values shown are for a frequency far removed from characteristic eigen frequencies of the electrons in these molecules. If the applied

frequencies are close to such an eigen frequency, the behavior of the polarizability will show the familiar dispersion behavior.

$$\alpha \propto f_i \left(\nu_i^2 - \nu^2\right)^{-1} \tag{2}$$

where α is the polarizability, f_i the oscillator strength, ν_i the eigen frequency, and ν the applied frequency. Clearly polarizability increases sharply near such frequencies.

2.2 Scatter Theory

Scatter of light by molecules of the atmosphere is given by the Rayleigh equation (4) where I_o is initial intensity and λ the wavelength.

$$I(\theta) = I_o NV (2\pi)^4 \lambda^{-4} \alpha^2 (2r^2)^{-1} (1 + \cos^2 \theta) \tag{3}$$

Intensity $I(\theta)$ is observed at a distance r at angle θ from a scattering volume V containing N scatterers per unit volume each of polarizability α. This polarizability term is not well known in the ultraviolet and requires some effort to determine. Polarizability of air can be obtained from the index of refraction, n, and the number density N by the relation:

$$\alpha = 3 (n^2 - 1) (4\pi N)^{-1} (n^2 + 2)^{-1} \tag{4}$$

While n increases with decrease of wavelength, values for n in the intermediate or short ultraviolet does not appear to be readily available. Penndorf's work on atmospheric scattering as tabulated in the Handbook of Geophysics (5) provides a means for determining polarizability through the relation:

$$K = 2.67 \tau (2\pi)^4 \lambda^{-4} N\alpha^2 \tag{5}$$

where K is the total scatter coefficient. When N is 2.55×10^{19} molecules cm^{-3}, the number density for standard sea level, this equation reduces to

$$\sigma = (1.733 \times 10^{-12}) \lambda^2 K \qquad (6)$$

Figure 1 -- Atmospheric Polarizability vs. Wavelength has been computed from the atmospheric scatter table (5). The dashed portion of the curve between 200 mμ and 185 mμ is an estimate of the sharp increase in polarizability due to the observed resonance fluorescence of O_2 at 184.9 mμ and 185.1 mμ. It is therefore clear that the intensity of scatter at any angle θ increases as wavelength decreases both from the λ^{-4} relation and the increase in σ.

Experiments to study scatter must also consider the atmospheric absorption coefficients. Of these coefficients, that of oxygen is the most important. Figure 2 gives oxygen absorption data for the shorter wavelengths at altitudes from 0 to 140 kilometers. The absorption coefficient k of this table refers to the radiation transmission equation

$$I = I_0 \, e^{-kx} \qquad (7)$$

where x is layer thickness in meters and I_0 and I are incident and transmitted intensities respectively. If we are concerned with total optical path lengths in the vicinity of four meters, a scatter intensity accurate to a few percent can be obtained by working with wavelengths where the absorption coefficient k is between .01 and .001. At sea level then the optimum wavelengths would be between .20μ and .24μ while above 60 km a band between .18μ and .19μ would be most useful.

A few simple calculations can now yield information as to the actual reflectivity of the atmosphere in the intermediate ultraviolet. If we

consider backscatter where θ is approximately 180 . equation (3) may be rewritten as a backscatter relation:

$$I_{(180)} = I_o r^{-2} V \eta \tag{8}$$

where

$$\eta = (2\pi)^4 \sigma^2 \lambda^{-4} N \tag{9}$$

Figure 3 shows the variation of η with altitude and for wavelengths 0.20 μ and 0.24 μ. The reflectivity at 0.18 μ to 0.19 μ will be considerably greater due to oxygen resonance fluorescence but has not been determined.

2.3 Solar Background

The optical system receiving the desired scatter radiation in any test conducted in the free atmosphere will also pass to the detector any other radiation falling within the operating wavelength band pass provided only that it arrives within the sensitive solid angle of the system.

Scatter experiments performed in daylight at various altitudes within the atmosphere must therefore consider the initial spectral distribution of the solar beam in space and its penetration through the atmosphere. Figure 4 sketches the spectral energy of the sun outside earth's atmosphere, Reference (6). Figure 5 gives the atmospheric penetration of this radiation as sketched by Friedman (7). If we wish to avoid solar background it is once again evident that scatter experiments must be performed at wavelengths shorter than about 0.24μ . Not only is solar irradiance quite low in these wavelengths but the atmosphere itself absorbs much of the incident energy. The wavelength band .20μ to .24μ can be shown to be suitable for altitudes below 60 km and the band .18μ to .19μ for altitudes above 60 km.

2.4 Mie Scattering

An ultraviolet densimeter will not be useful when operated within the troposphere due to the widely varying density of particles with sizes comparable to the wavelengths of the ultraviolet used or larger. In general the total scattering coefficient from N spheres of radius R in unit volume is

$$k = N\pi R^2 f(2\pi R \lambda^{-1}) \qquad (10)$$

and as stated by Condon (4) $f(2\pi R \lambda^{-1})$ approaches $(2\pi R \lambda^{-1})^2$ when particle radii are about $(2\pi)^{-1}$ of the wavelength. Backscatter is a maximum with this situation. For example particles with a 0.032μ radius would have a reflectivity of about 10^{-11} per particle when illuminated by 0.2μ radiation. This is about the reflectivity of the atmosphere at 85 km. see Figure 3. To judge the possibility of such density at very high altitudes. we note that 80-85 km is the altitude at which noctilucent clouds occur. These clouds are quite rare and appear to have particle densities in the vicinity of 10^{-2} cm^{-3} for radii around 0.1μ. Ludlam (8); Witt (9), so that even when operating a ultraviolet densimeter in a noctilucent cloud one could expect the backscatter signal from the air molecules to be 10 to 100 times that from the cloud particles. The other high atmospheric region which accumulates dust would be the lower stratosphere in vicinity of 20 km. According to Junge (10) the $.1\mu$ to 1μ particle densities here may be in the order to 1 cm^{-3} or a reflectivity of 10^{-10} cm^{-1} but the atmospheric scatter at this altitude is at least a factor of 200 times that from the dust. One can conclude that above the tropopause Rayleigh or resonance scattering will predominate over particulate scattering except on rare occasions such as caused by volcanic or nuclear explosions.

3.0 BACKSCATTER INSTRUMENTATION

The measurement of ultraviolet backscatter from a vehicle which is moving through the atmosphere and surrounded by shock wave and boundary layers requires special considerations in the design of its transmitter and receiver. The transmitter should have a relatively narrow beam so that the illuminated volume may be precisely located at any selected distance. The receiver should be optically focussed on the desired scatter volume and should use field stops to cut off radiation from other angles. The receiver must be equipped with efficient optical band pass filters or detectors so that response to the intense portions of the solar spectrum is practically zero.

3.1 Ultraviolet Transmitters

The ultraviolet sources developed for the project borrowed largely from previous experience at Plasmadyne and from the work of Fischer (11, 12). Figure 6 sketches the three transmitter geometries which were studied. Type 1, the orifice spark transmitter, utilizes plate electrodes separated by an insulating material and then drilled to locate a small spark orifice. Type 2, the pointed electrode transmitter, is more conventional and uses a reimaging mirror and lens. Type 3, the most efficient and highest powered unit developed, is the parabolic reflector type. All of these transmitters were built with gas tight seals and are pressurized with argon at 35 psig.

Our first work considered observation of backscatter from fairly short distances, approximately 10 cm to 50 cm. Because of the advantage to such experiments if the probing beam is small and precisely located, the orifice spark transmitter, type 1, was studied. Its radiation source is very

small and with a lens produces a well collimated beam. Two techniques which can confine a spark discharge to a 0.25 mm orifice and thus eliminate positional jitter, were studied. One technique used a gas vortex flow between two closely spaced flat electrodes exhausting through an axial aperture in one of the electrodes. With this technique the vortex gas acts as the insulator. Even at low gas flows the spark discharge occurs along the low pressure axis of the vortex within the small orifice. The second technique employed two flat plate electrodes separated by a thin wafer of dielectric material. A 0.25 mm diameter hole was drilled through one electrode and the insulator. With the application of a sufficient voltage a spark discharge will occur through the small aperture. Rechargeable nickel cadmium batteries, a simple 24 V DC to 5 KV DC converter, a pneumatic or rod operated microswitch for on-off, and a low inductance capacitor for spark energy storage completed the initial ultraviolet beam unit. The best of these spark units used a tungsten back electrode, a zirconium oxide dielectric wafer and a molybdenum front electrode with 0.25 mm diameter discharge aperture. This unit, using discharges of 0.03 μf at 5 KV or a pulse energy of 0.38 watt second has a 23 minute life when firing at 5 pulses per second. The vortex gas flow type has a much longer life but was not studied extensively as it must use a recirculating pump. The additional weight and power requirement seemed unrealistic for sounding rocket flights.

The study of spark radiation sources immediately involves radio frequency noise problems. Shielding in the transmitters is accomplished by using ferromagnetic enclosures. The only openings to the shielded

transmitter units are a connector at one end for battery voltage check and charge, an opening for a pneumatic tube or lucite rod activating an internal microswitch, and an opening for the light beam at front of the unit. RF electromagnetic radiation from the spark circuitry is thus reduced to very low levels.

The beam cross section produced by these type I units at one meter was examined by means of an RCA 1 P28 photomultiplier with an 0.37 mm aperture before the photo cathode. At one meter distance the width between 50% of peak intensity levels of a beam produced by a simple plano-convex lens or doublet will be a function of both wavelength band width and the distance from lens to source. Figure 7 shows measurements using fused silica lenses of about 4 cm focal length. Figure 7a sketches the broad beam resulting when the lenses are combined in a doublet with an effective focal length of 2.4 cm and without filtering. Figures 7b and 7c show the improvement due to placing a Corning No. 9863 filter before the photomultiplier aperture and due to using a single lens at greater distance from source. Figure 8 displays the band pass of the No. 9863 filter. Figure 9 is a sketch showing the shape of the transmitter UV pulse as seen by oscilloscope. The half intensity duration of the main pulse is 0.13μs. The radiation from this source approximates a 40,000 K black body in spectral distribution up to the vacuum ultraviolet. Figure 10 displays the distribution of energy from a 40,000 K blackbody down to 0.18μ; it is probable, however, that the sharp peak will show line structure depending on gas and electrode materials in any actual spark source. Figure 11 sketches the transmittance of fused silica from two manufacturers and indicates that this material

may be used with spark UV radiation source wavelengths as small as 0.18μ.

A special RCA photomultiplier, C 7180 C with a CuO photocathode was used for the testing of source intensities in the intermediate ultraviolet. Figure 12 gives the response of this tube. The CuO bandpass would be almost ideal for the instrumentation of this project but considerably shorter optical paths would have to be used since, unfortunately, the quantum efficiency of the CuO surface is very low. At wavelengths below 0.2μ, atmospheric absorption becomes important at sea level densities. Oxygen absorption is particularly important having absorption coefficients per meter of 39.8 at 0.18μ, 1.99 at 0.19μ, 0.0199 at 0.20μ and 0.0078 at 0.21μ. See equation (7). Clearly, the shorter wavelengths in the response of the RCA C 7180 C cannot be utilized over meter distances without reducing the optical path-density.

Study of intermediate ultraviolet radiation from various electrode materials with argon as the working gas was also accomplished by use of the RCA C 7180 C photomultiplier. We had expected materials like hafnium carbide, magnesium and europium to be the best emitters. However, two tungsten electrodes with argon produced the most intense radiation. Probably the argon becomes opaque at the vicinity of its lines 0.163μ to .168μ in view of the spark pressure and temperature, while the continuum in the near ultraviolet does not quite reach black body conditions. It was also noted that the ultraviolet beam diameter at half peak intensity level and one meter distance was only 7.6 mm for the tungsten argon combination.

The second ultraviolet transmitter developed, type 2, used two transverse electrodes with a reimaging mirror and a collimating lens as shown in Figure 6b. This design allows light pick-up over about 0.8 steradian and thus emits considerably larger pulse energy. The cylindrical capacitor used for energy storage was increased to 0.3 μf and the spark gap adjusted to fire at 5000 volts for a pulse energy of 3.7 watt seconds and duration of one microsecond. The ultraviolet beam energy of type 2 units is therefore more than ten times that of the type 1 orifice units. At the same time the life of the type 2 unit is much longer since electrode wear is slow and the limiting factor in any run is a slow clouding of the lens surface by finely divided electrode material. Runs of over one hour at 5 pulses per second have been achieved before the necessity of cleaning the lens and readjusting electrode spacing. All of the flight backscatter data was obtained with a type 2 unit. For flights the lens-spark spacing was adjusted to give a minimum beam diameter at 2 meters. At wavelengths between 0.23 μ and 0.25 μ the beam diameter at 2 meters is 5 cm.

Type 3, the third ultraviolet transmitter developed, uses a polished aluminum reflector with a parabolic figure as shown in Figure 6c. This deep parabola collimates about 8 steradians of the spark energy and its beam energy per pulse when using 4 watt second discharges is about ten times that of the type 2 rod electrode unit. The inductance is a little higher so that pulse duration is about 2 microseconds. Figure 13 is a photograph of the parabolic ultraviolet transmitter. The UV beam has a diameter of 8 cm at the exit aperture and 12 cm at 10 meters. These dimensions are, of course, the same for all wavelengths. When used in backscatter instrumentation the

parabolic transmitter must be located at a greater distance from the receiver due to the larger beam diameter. The type 3, or parabolic transmitter, is the most effective of those transmitters developed but unfortunately it was developed too late in the program for flight tests.

All of the ultraviolet transmitters are equipped with means for monitoring the output pulse energy. The orifice spark and the rod electrode units have a small post reflector just outside the collimating lens to send a portion of the pulse to a phototransistor mounted at the side of the transmitter. The parabolic reflector unit has an opening at the side of the enclosing fused silica plate which leads to a phototransistor. Sufficient scatter occurs within the plate to fill this side opening with radiation. In each case a small filter disk of Corning 9863 is placed in the optical path so that the phototransistor responds to the ultraviolet as shown in Figure 14. The monitored wavelengths therefore peak at around 0.35 μ while the scatter signal should be observed in wavelengths near 0.2μ . To eliminate this mismatch a phototransistor with a fused silica window and a small intermediate ultraviolet band pass filter are required. Neither were available.

The high voltage power supply for all of the ultraviolet transmitters is constructed so that most of the unit plugs with a cylindrical energy storage capacitor. Figure 15 sketches the circuit employed. The battery or external power is first regulated by a Zener diode circuit and then used to run a ringing choke DC-DC converter. The spark unit works as a relaxation oscillator with the firing rate determined by the spark gap

adjustment and the power and voltage capability of the power supply.

3.2 Ultraviolet Receivers

The essential components of the ultraviolet receiver are the radiation collecting component and the detector. Considering the proposed uses of the densimeter on rockets, missiles, or re-entry vehicles, and the decision to use the intermediate ultraviolet, only two materials appear feasible, fused silica and sapphire. On cost considerations, fused silica was selected and a double convex lens of 9.4 cm diameter and 14 cm focal length at 0.2 micron is used as the receiver objective. The field stop at the plane were radiation from the scatter volume is imaged may be an aperture or it may be the actual sensitive surface of the ultraviolet detector.

The multiplier phototube has the highest quantum efficiency of any ultraviolet detection device for which we were able to obtain information, also they characteristically have megacycle response. The RCA 1P28 is typical of these tubes. The 1P28 uses a Cs-Sb photocathode, has a 15% or greater quantum efficiency in the UV and has an envelope of high silica glass with a good spectral response extending to 0.19 μ, (13). Coupled with an efficient and solar blind band pass filter this tube would be excellent for atmospheric backscatter experiments. Figure 16 gives a typical quantum efficiency curve.

Figure 17 sketches the median amplification of an electron leaving the photocathode of the 1P28 and moving through the dynode structure for various supply voltages. These amplications are sufficient to give pulse outputs varying from a few microamperes to a few milliamperes in the scatter experiments. The output can vary over a range of 10^3 without damage when using a constant supply voltage. These conditions imply that for the rocket backscatter experiment with its required range of 10^6, one must either use a variable supply voltage or a constant supply voltage with a variable entrance aperture. Considering reliability, a precisely stepped supply voltage controlled by the output signal would be possible without resorting to mechanical devices. The variable aperture would offer a lower noise level within the photomultiplier but would require a mechanical device.

A number of conventional solar blind photomultipliers were tested, but while "solar blind" their quantum efficiency was so low in the intermediate ultraviolet that use in backscatter instrumentation was not feasible.

Photomultiplier tubes under more recent development were then investigated. Of these RCA's C70127 using a cesium telluride photocathode was selected. The quantum efficiencies of these tubes varies with the individual unit and Figure 18 sketches the approximate efficiencies of the tube in use. It is not quite "solar blind" in the low atmosphere due to response at 0.3 μ . The photomultiplier uses 12 dynodes which are

relatively insensitive since for a supply voltage of 1500 volts, the dynode gain is 130,000. The C70127 is quite small as shown in Figure 19. For densimeter operation the CsTe C70127 was potted with RTV silicone rubber inside a stainless steel cylinder. The divider and load resistors with pulse smoothing capacitors were soldered directly to the flexible leads and potted in epoxy resin as a step toward easing vibration loads on the photomultiplier.

3.3 Ultraviolet Band Pass Filters

The necessity of obtaining high quantum efficiency detection of intermediate ultraviolet photons in the presence of sunlight poses a difficult problem. One solution is to find a spectrally selective photodetector and use additional filtering to shape the desired band pass. The other is to use a reliable and rugged tube with very wide spectral response such as the 1P28 and do the entire band pass shaping by filter. We were unable to locate a filter of this type. Interference filters, solutions, films on quartz, etc., were studied and in some cases tested but without success. Finally, a gas cell filter using about 6 cm STP of chlorine between fused silica windows was constructed. Figure 20 gives the transmission of this cell. The 0.4 to 0.5 transmission between 0.22 μ and 0.25 μ and sharp cutoff between 0.27 μ and 0.29 μ makes this an excellent filter for use with the cesium telluride photomultiplier, see Figure 18. The filter transmission in the blue is not significant as the cesium telluride tube does not respond at these wavelengths. Tests of this combination in sunlight show little solar noise unless pointed directly at the sun. Apparently filtering out all solar photons is extremely difficult. Referring

to Figure 5, atmospheric penetration of solar radiation, a densimeter using a CsTe photomultiplier and chlorine filter should be effective to 35 or 40 kilometers altitude. For higher altitudes the band pass should be shifted toward shorter wavelengths.

3.4 Signal Amplifying Circuits

A number of amplifier techniques can be used with the pulsed ultraviolet densimeter. The best solution depends on how the output signal is to be displayed and for what purpose the data is intended. For example, if the data is to be viewed on a meter dial, as an indication of density a circuit dividing the smoothed output of the scatter amplifiers by a smoothed signal proportional to the output ultraviolet energy would be satisfactory. The time constants and the pulsing rate can be selected to match the specified rate of altitude change. On the other hand for an experimental program where the effects of solar background and reactions between the densimeter and the vehicle are partially unknown it is better to amplify and record each pulse separately. The data circuits developed in the project are of this experimental type.

In our units the photomultiplier acts as a first stage in the detection portion of the amplifier. Figure 21 gives the entire photomultiplier circuit from a 16.4 v regulated input power (see Figure 22) to an emitter follower transitor delivering the input pulse signal to pulse amplifying and stretching amplifiers. The regulated line power first goes through a second regulator with a zener reference diode which acts as the final control over the high voltage applied to the photomultiplier (RCA's C70127).

A ringing choke DC to DC converter is used to step 6.7 volts at the zener to 1350 volts over the photomultiplier. Magnetic shield cans are used to separate the DC-DC converter from the rest of the circuit, so that its kilocycle ring is not picked up by the photomultiplier circuit. The microsecond scatter pulse entering the phototube is then linearly amplified and appears across the 1200 ohm load resistor terminating this portion of the data circuit.

The voltage pulse at the photomultiplier load resistor is transmitted by capacitor to three amplifiers as sketched in Figure 23. The gains of these circuits are adjusted so that if the high sensitivity channel gain is A_m then the medium sensitivity channel gain is $A_m/10$ and the low sensitivity channel is $A_m/100$. All three amplifiers begin with tuned emitter transistor stages. The high sensitivity channel has three transistors, the medium gain two and the low gain amplifier one. The tuning was done to give maximum response to pulses of about one microsecond duration or in other words to pass the scatter pulse. The frequency of occurrance of noise pulses of sufficient amplitude to affect these circuits is much greater at low input signal levels than it is at high. This difficulty was met by using a more sharply tuned band pass in the high gain circuit. After passing the tuned emitters the signal passes through slower and slower transistors until finally charging a 5 μf capacitor through a diode. The capacitor voltage is then related to the amplitude of the scatter pulse initiating the amplifying provess. The capacitor signal voltage is connected by a high impedance circuit of two transistors to a 10,000 ohm load resistor. These load resistors have the final output

signal and may be observed by any compatable recording or telemetering device.

Study of the circuit diagrams will show that each 5 μf signal capacitor is connected to the negative lead through a silicon controlled rectifier of very high resistance so that the time constant for each capacitor discharge is large. The silicon controlled rectifier is triggered into conduction by pulses from a timing circuit shown in Figure 24. As we discussed in the section on ultraviolet transmitters, the output pulse must be monitored to take care of amplitude jitter, and slow changes due to electrode erosion. A phototransistor with a Corning 9863 filter is used as shown in Figure 25. The phototransistor pulse caused by a very small portion of the output beam is amplified and used to charge a capacitor for an output signal just as in the other three output circuits dealing with scattered radiation. However, this phototransistor signal in addition starts a conventional one-shot multivibrator in conjunction with a uni-junction transistor. At 100 milliseconds after the phototransistor pulse the timing circuit generates a pulse which triggers all four silicon controlled rectifiers into conduction and thus all charged signal capacitors are discharged and remain in this state until the next pulse is received. Figure 26 gives flight data as recorded on 21 January 1963 at about 1140 pst. Looking first at the 800 meter recording , we see that the low gain scatter data is at the top. The 100 millisecond pulses with their slowly tapering tops are displayed as they occur during 5 seconds from left to right with pulsing at the rate of a little more than 5 per second. Just below are pulses showing the ultraviolet transmitter output pulse, then the output of the high gain

and finally the medium gain channel. The medium and high channels are overloaded with a maximum signal while the low gain channel occasionally overloads at the edge of the recorder film. The amplitude jitter of the ultraviolet source is very evident and, of course, demonstrates the need for monitoring its intensity. The capacitor charging type amplifier is not quite linear as is shown by Figure 27. The S shaped response is generally characteristic. This variation must be considered in reducing the experimental data.

3.5 Backscatter Geometry

The ultraviolet densimeter receiver and transmitter can be located to give an intersection volume in a number of ways. Figure 28, backscatter geometry, assumes that the transmitter and receiver beams are of about the same cross section and are collimated to a few degrees. Because the scattered radiation returned to the receiver varies with the reciprocal of distance squared the bulk of the pulse energy returned is from the scatter volume between first intersection of the beam and the distance ℓ_a where the axial lines of the beams intersect. It is clear that if the receiver and transmitter are close together the scatter volume is a maximum, but the distance to the individual scatterers varies widely. If the two units can be separated so that their beams form a 90° angle, the scatter volume is closely located, but its volume is a minimum. Also referring to equation (3) of section 2.2, the actual scatter intensity per unit volume is decreased by a factor of 2 because of the $(1+\cos^2\theta)$ term. When mounted on any given vehicle, the geometry selected will have to depend on the application.

4.0 FLIGHT TESTS

The vehicle planned to carry the developed ultraviolet densimeters varied during the course of the project. Originally the assigned vehicle was an Aerobee Hi rocket, but due to work load difficulties this flight was postponed. The second vehicle selected was the F-104 aircraft. The altitude possible is much less than with the rocket, but problems of flight qualification and daytime operation can be solved more easily when repetitive flights are possible. The F-104 flights have allowed demonstration of the feasibility of this type densimeter.

4.1 Proposed Aerobee Flights

The proposed installation of an ultraviolet densimeter in the first straight housing section after the nosecone of an Aerobee Hi Rocket is sketched in Figure 29. The receiver is adjustable so that the scatter volume can be centered either at 1 meter or 1 5 meters from the housing skin. By these adjustments the scatter volume can be located in the ambient atmosphere outside shockwaves both with a nose probe and with a normal nose. Figure 30 sketches actual shape of the ultraviolet densimeter as it was to be mounted in the Aerobee and shows the essential internal components. The battery packs were built up using Yardney Silvercels in separate magnetic shield cans for receiver and transmitter. Figures 31 and 32 give an expanded component view and a front view of the ultraviolet transmitter. The tubing sections are O-ring sealed at the end caps and the rear housing. The tubes are charged with dry nitrogen at 35 psig. The top expanded component line in Figure 31 shows the location of

fused silica transmitting lens, spark UV source, co-axial capacitor, DC-DC converter, along with magnetic shield cans and housing. The lower expanded line shows the batteries and their holder. An on-off switching solenoid is visible between the two component lines. The switch was to be turned on as the rocket flight began. Figures 33 and 34 show an expanded view and front view of the ultraviolet receiver. The large receiving lens is followed by a glare stop and field stop and in this photograph the light passes through an interference filter to a EMI 6256 BN photomultiplier carried within an aluminum can which is at photocathode potential. The pulse expanding amplifier is clustered around the photomultiplier. The receiver unit is switched on and off by a solenoid which closes a double pole micro-switch located in the battery-tube. The complete ultraviolet densimeter rack mounted much as it would be in a rocket is shown in Figures 35 and 36. Figure 37 is a photograph of the densimeter as set up for outside daylight tests at Santa Ana.

4.2 F-104 Flights

Flight test of the ultraviolet densimeter was not accomplished in the Aerobee and instead it was decided to test in F-104 aircraft based at the NASA Flight Research Center, Edwards, California. Environmental tests for aircraft flight conditions were then conducted. Altitude tests posed no problems as the units were pressurized with dry nitrogen so that external pressure changes were not important. Shake tests quickly showed that the microswitches planned for use in turning the battery power on and off for the Aerobee flight chattered under aircraft operating conditions. Also, the rechargable battery system with Yardney Silvercels was not

practical under a testing program. One cannot stop to charge batteries every 15 or 20 minutes. It was therefore decided to use external battery packs for both transmitter and receiver. This change also eliminated the microswitches. Additional noise problems were, of course, inevitable with the batteries outside the magnetic shield cans. However, line filters were constructed which solved this problem. Figure 38 gives an oscilloscope photograph showing the various channel outputs with the receiver lens covered after the modifications were accomplished. Only the high gain channel shows an RF spark pulse pick-up and this is quite small compared to the scatter signals to be measured.

Temperature environment tests quickly showed that the amplifier outputs were temperature sensitive even after elimination of some of the difficulty by use of thermistors. It was decided to use thermostat controlled heater blankets to meet this problem.

Figure 39 is a photograph of the ultraviolet densimeter with heater blankets installed and mounted on a rack for installation within the F-104 nose. The rectangular box at the side of the transmitter tube houses the phototransistor and its amplifier. Figure 40 shows the densimeter mounted within the nose, and Figure 41 is an external photograph clearly showing the transmitter and receiver lenses.

The most successful flight of this equipment was achieved near noon on 21 January 1963 when data to 10 kilometers altitude was achieved. Figure 42 gives a plot of the reduced data. This data was reduced point by point

averaging the output for five pulses for a resolving time of one second and compared to radiosonde data taken at approximately the same time. Due to lack of calibration for the densimeter the reduction equations were adjusted so that the radiosonde data and UV densimeter data were essentially equal at the 9.7 km maximum altitude where the Rayleigh scattering would predominate. The two curves show close agreement down to 4 kilometers. Below this altitude Mie scattering becomes increasingly important. The airmass envolved was of fairly recent polar maritime origin with a temperature of -49 C at 10 kilometers and was very clean at this altitude. It is interesting to note the increased scatter below 4 kilometers even under these conditions. At 9.7 kilometers and a density of .435 kg m^{-3} the low gain channel was still operating. This means that a similar signal would exist on the high gain channel at a density of .00135 kg m^{-3} or at 39 km in the ARDC standard atmosphere. The signal would be more noisy due to the reduction in number of scatter photons but this effect could be compensated for by using a longer resolving time or by increasing pulse repetition rate.

The successful flight used a chlorine gas filter and a cesium telluride photomultiplier which represent the best solar blind scatter detection combination achieved to this date. However, shortly after the flight data presented here was taken the chlorine filter cell began leaking, allowing solar photons to reach the photocathode and impairing the remainder of the data. Since January 1962, the project has been slowed by difficulty in obtaining chlorine filter cells which remain sealed under flight conditions.

5.0 CONCLUSIONS

Investigative study and flight tests indicate that the ultraviolet densimeter based on Rayleigh scatter can determine the density of the ambient atmosphere surrounding a high speed vehicle. These density measurements can be performed at distances up to several meters from the vehicle even in daylight. Calculations show that if efficient ultraviolet bandpass filter and photodetector combinations were available this density measurement could be made from the tropopause, the beginning of the Rayleigh scatter atmosphere, to about 100 kilometers altitude, the limit of the homogeneous atmosphere.

6.0 REFERENCES

1. 1959:ARDC Model Atmosphere, Handbook of Geophysics, The MacMillan Company, 1-13
2. Hulburt, E.O., 1937: Observations of a Searchlight Beam to an Altitude of 28 km., J. Opt. Soc. 27, 377-382.
3. Friedland, S.S., Katzenstein, J., Sherman, J., and Zatzick, M.R., 1956: Improved Instrumentation for Searchlight Probing of the Stratosphere, The University of Connecticut.
4. Condon, E.U., 1958: Molecular Optics, Handbook of Physics, New York, McGraw-Hill, 6-124.
5. 1960: Thermal Radiation, Handbook of Geophysics, The MacMillan Company, 16-22.
6. 1960: Thermal Radiation, Handbook of Geophysics, The MacMillan Company, 16-16.
7. Friedman, H., 1960: The Sun's Ionizing Radiations, Physics of the Upper Atmosphere, Academic Press, 134.
8. Ludlam, F.H., 1957: Noctilucent Clouds, Tellus, 9, 341-364.
9. Witt, G., 1960: Polarization of Light from Noctilucent Clouds, J. Geophys. Res., 65, 925-933.
10. Junge, C.E., and Manson, J.E., 1961: Stratospheric Aerosol Studies, J. Geophys. Res., 66, 2163-2183.
11. Fischer, H., 1957: Simple Submicrosecond Light Source with Extreme Brightness, J. Opt. Soc., 47, 981-984.

6.0 REFERENCES

12. Fischer, H., 1958: Upper Temperature Limits in the High Pressure Discharge. Conference on Extremely High Temperatures. New York, John Wiley and Sons. 11-27.

13. Dunkelman, L., and Lock, C., 1951: Ultraviolet Spectral Sensitivity Characteristics of Photomultipliers Having Quartz and Glass Envelopes. J. Opt. Soc., 41, 802-804.

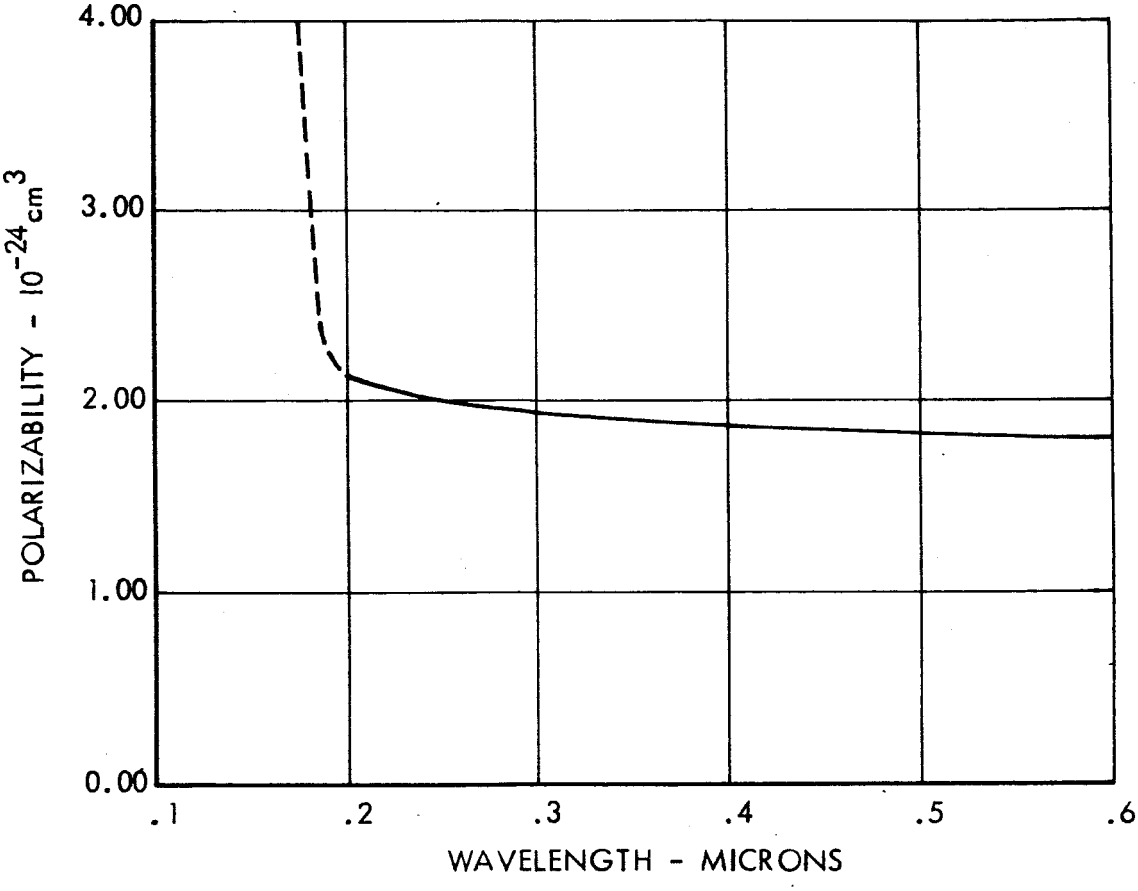

FIGURE 1 - ATMOSPHERIC POLARIZABILITY vs. WAVELENGTH

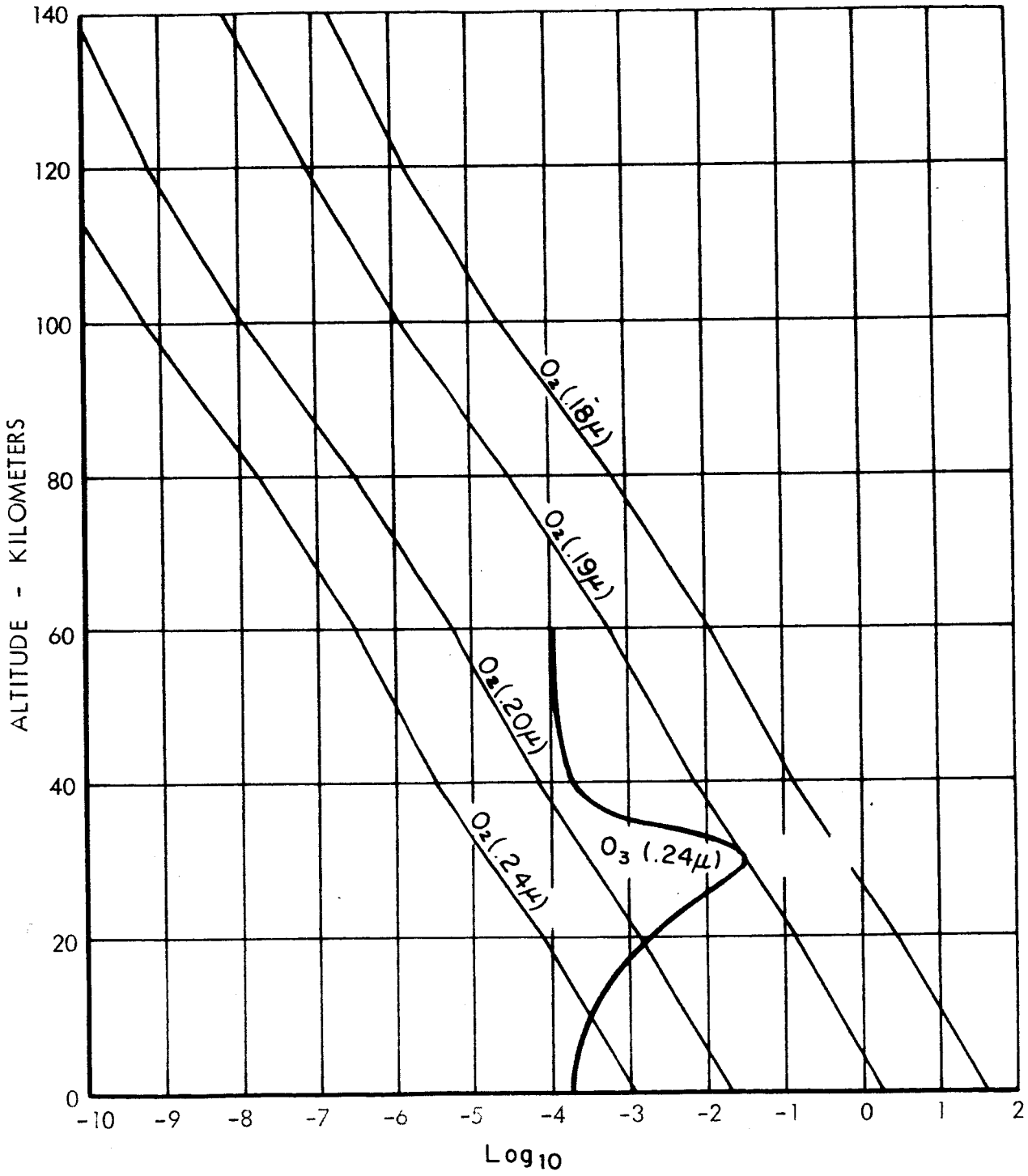

FIGURE 2 - ABSORPTION COEFFICIENTS for OXYGEN

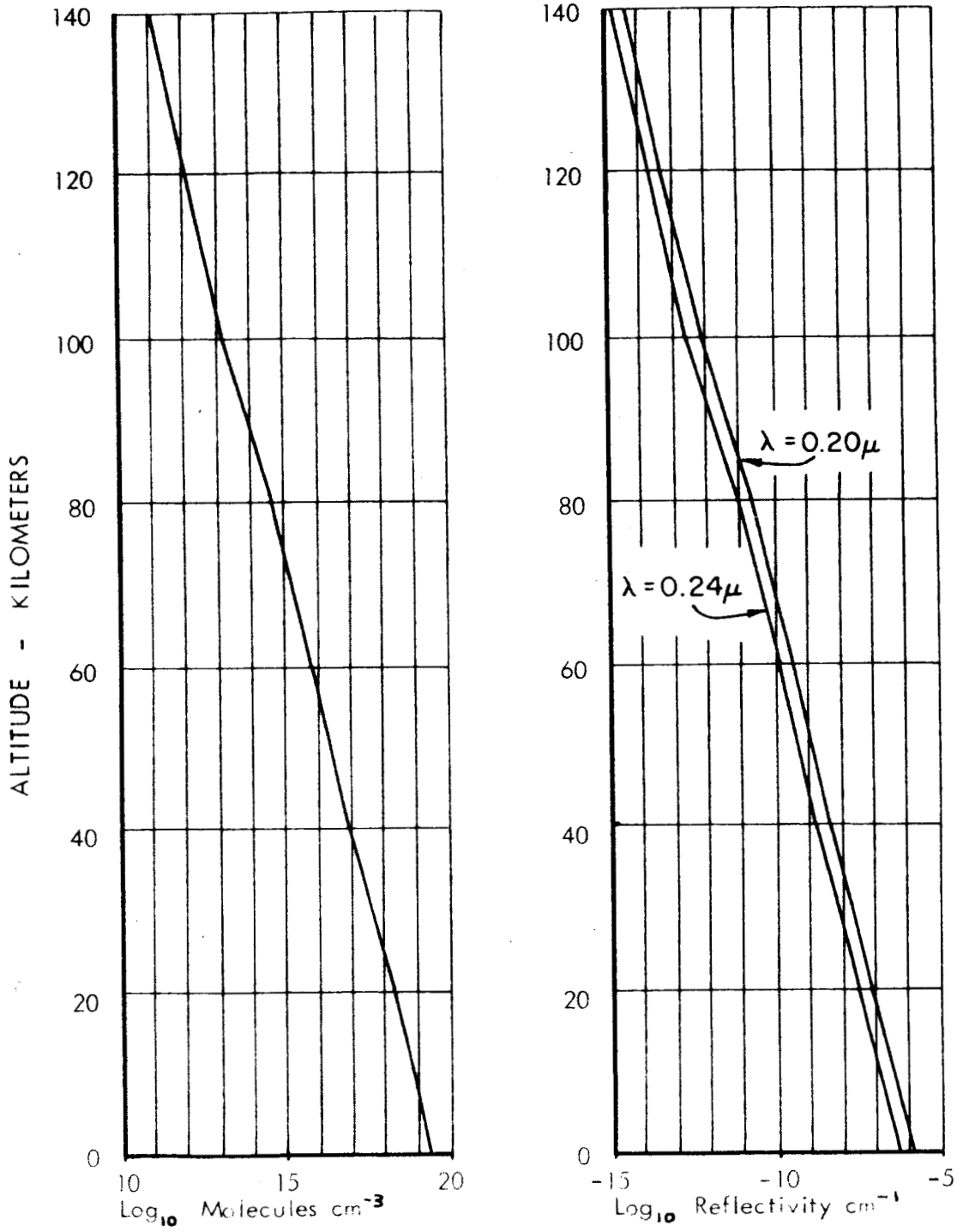

FIGURE 3 - η ATMOSPHERIC REFLECTIVITY

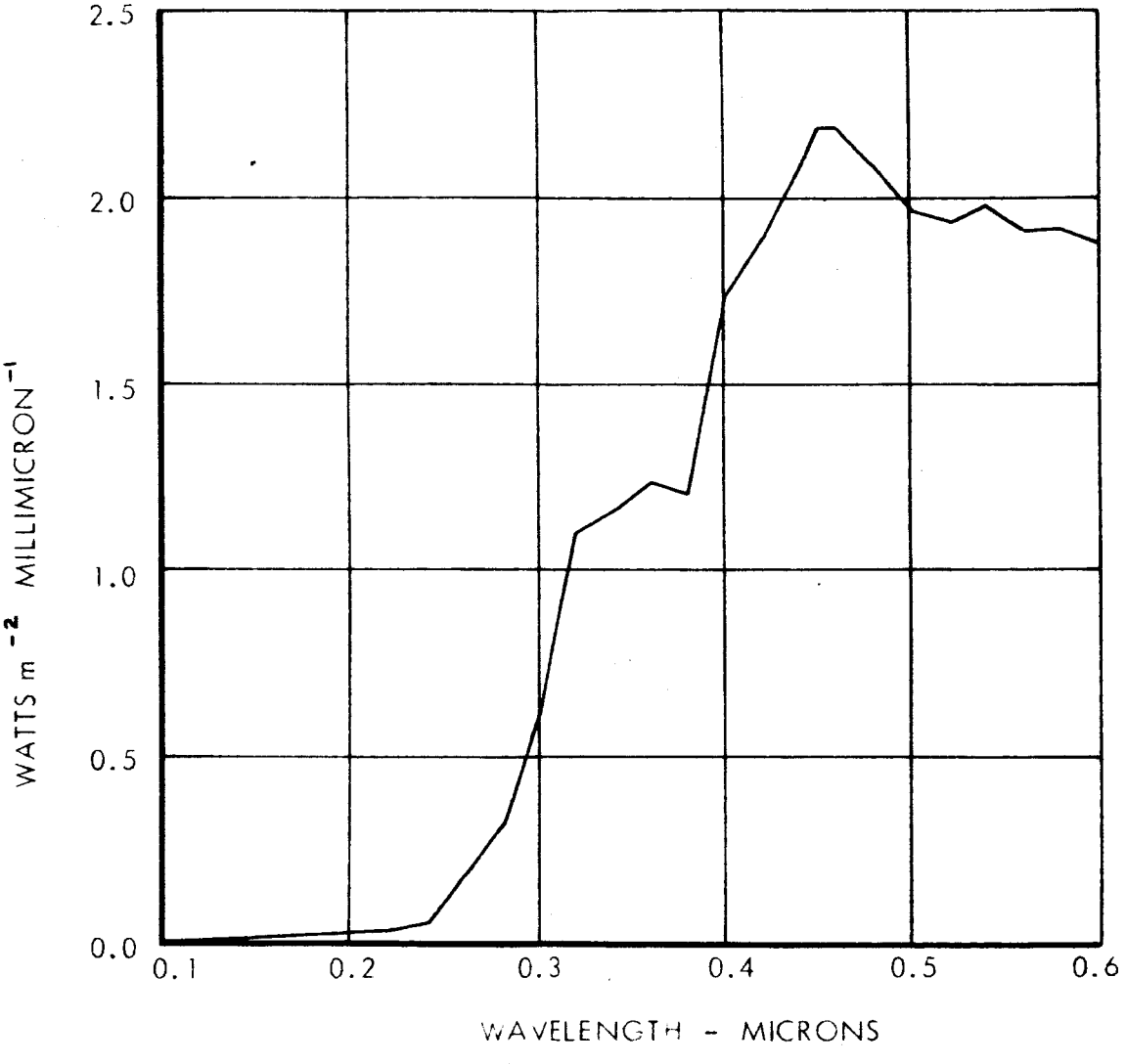

FIGURE 4 - SPECTRAL IRRADIANCE OF SUN OUTSIDE EARTH'S ATMOSPHERE

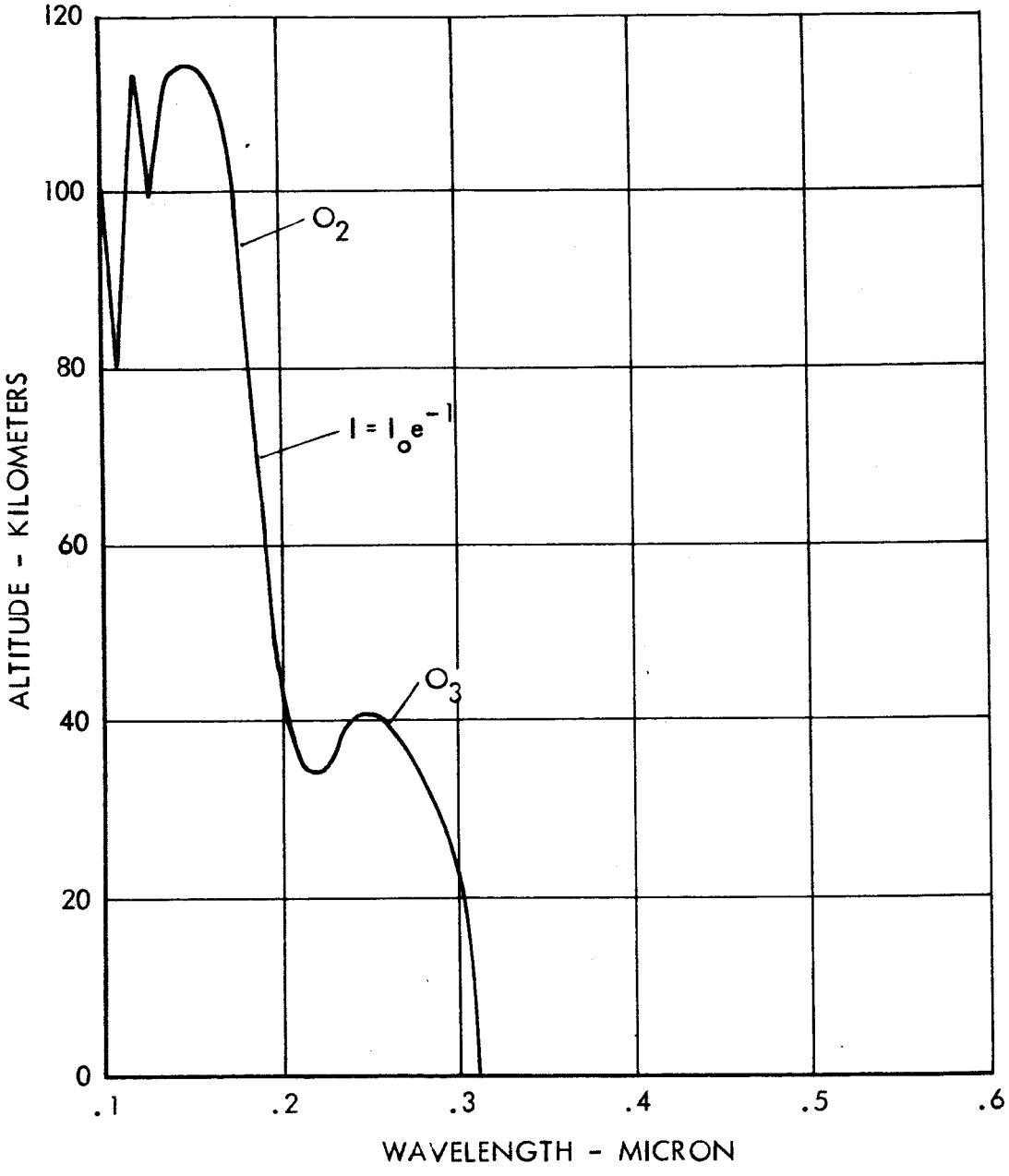

FIGURE 5 - ATMOSPHERIC PENETRATION OF SOLAR RADIATION

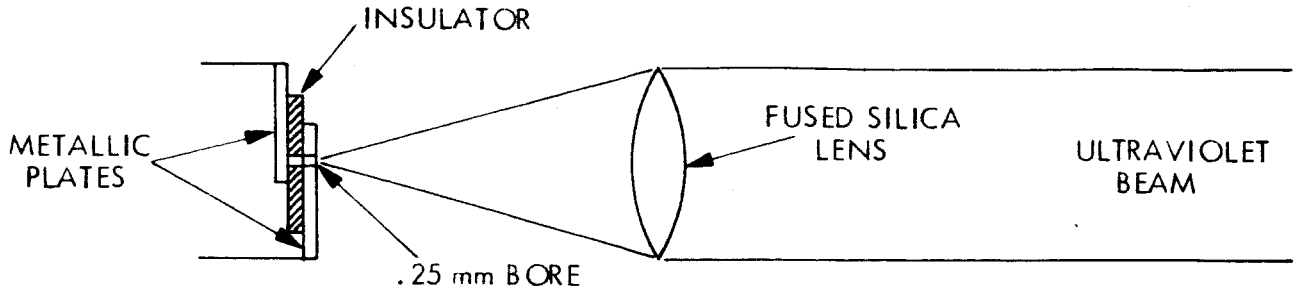

a) -. TYPE 1, ORIFICE SPARK TRANSMITTER

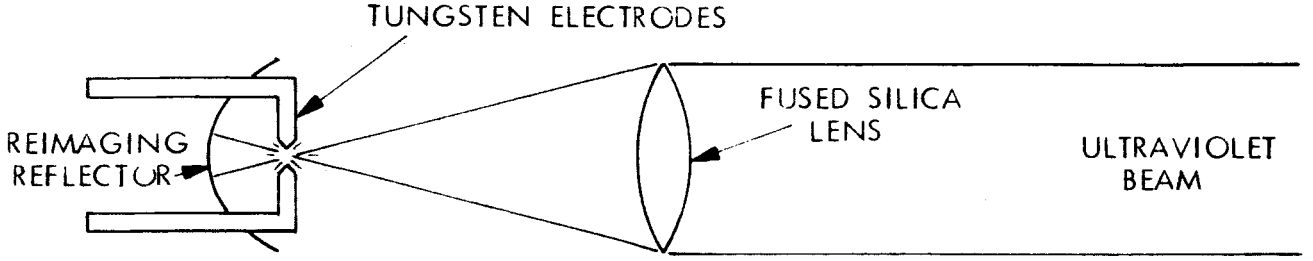

b) - TYPE 2, ROD ELECTRODE TRANSMITTER

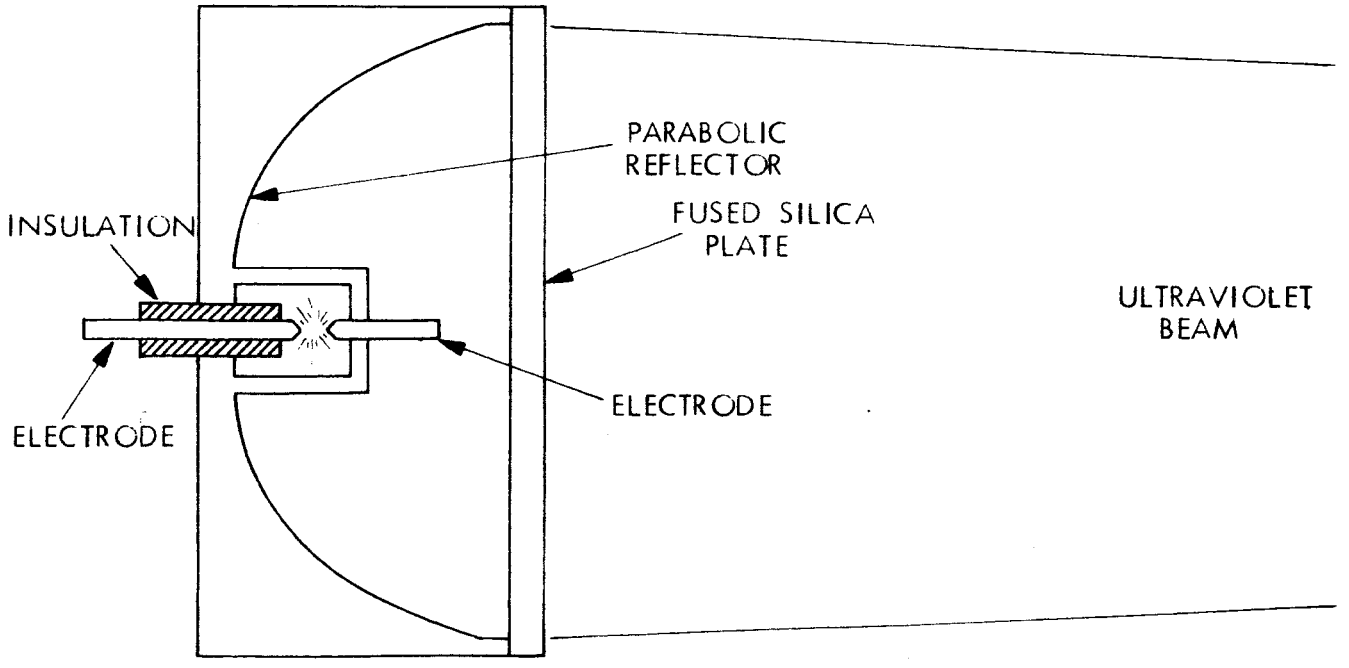

c) - TYPE 3, PARABOLIC REFLECTOR TRANSMITTER

FIGURE 6 - ULTRAVIOLET TRANSMITTERS

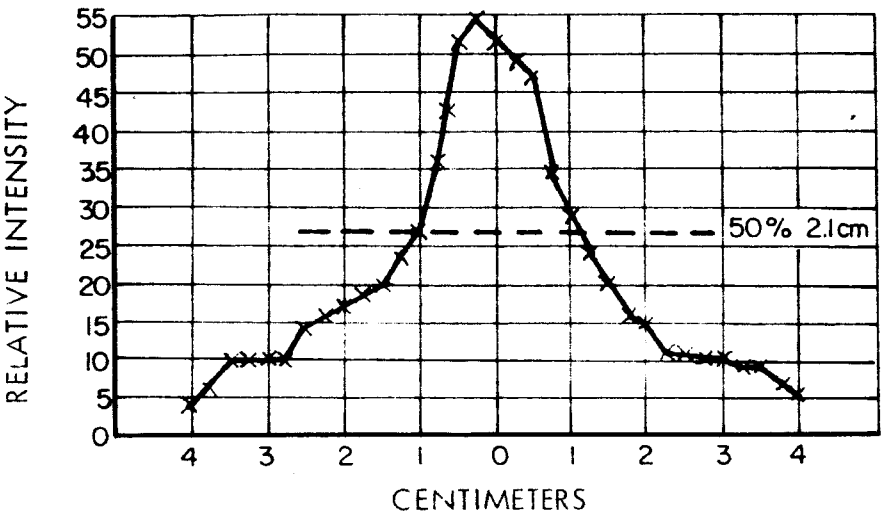

a) -- FUSED SILICA DOUBLET UNFILTERED 1 P 28

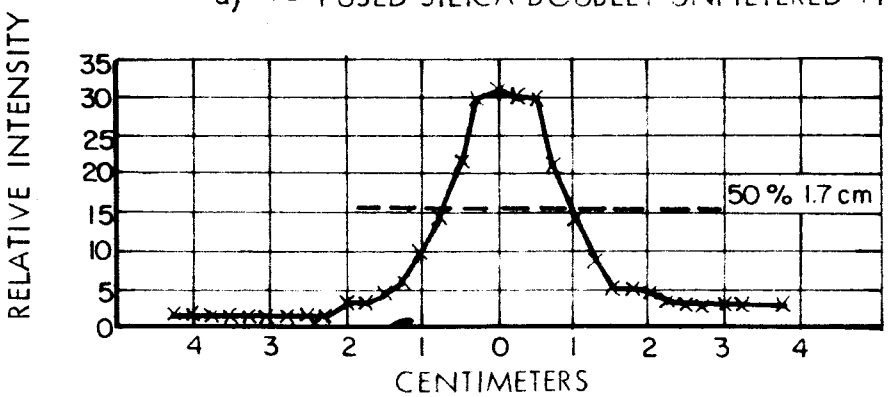

b) -- FUSED SILICA DOUBLET CORNING FILTER # 9863 1 P 28

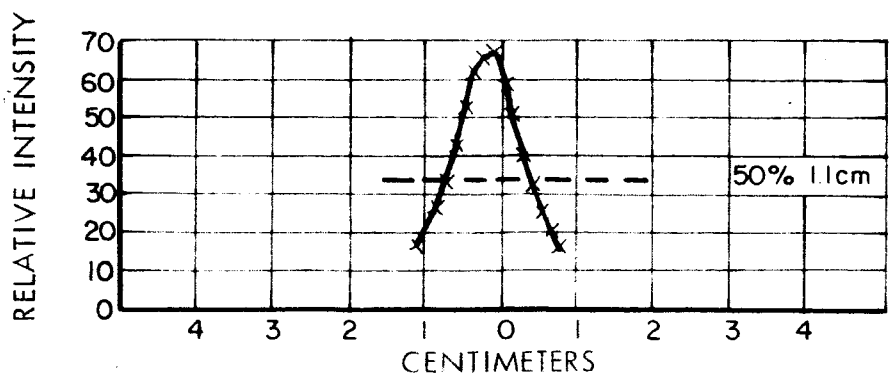

c) -- SINGLE FUSED SILICA LENS CORNING FILTER # 9803 1 P 28

FIGURE 7 - BEAM CROSS SECTIONS AT ONE METER FOR TYPE 1 UNITS.

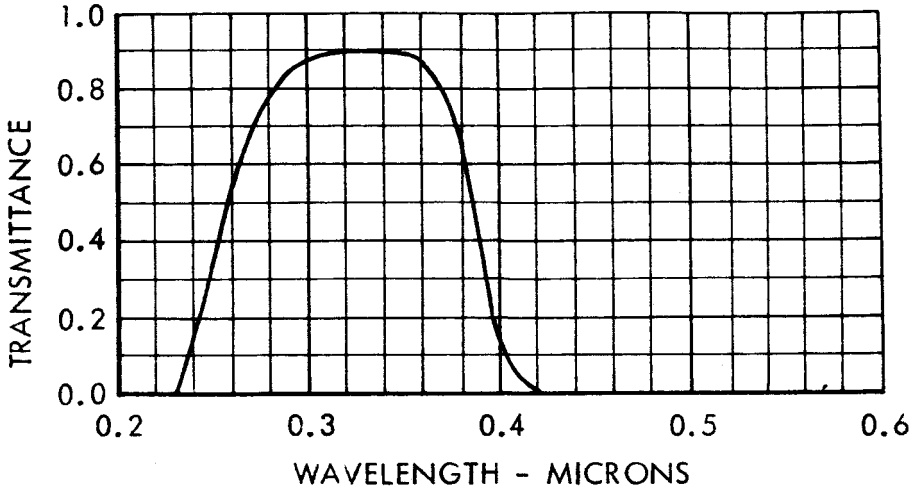

FIGURE 8 - CORNING FILTER # 9863 (3 mm thick)

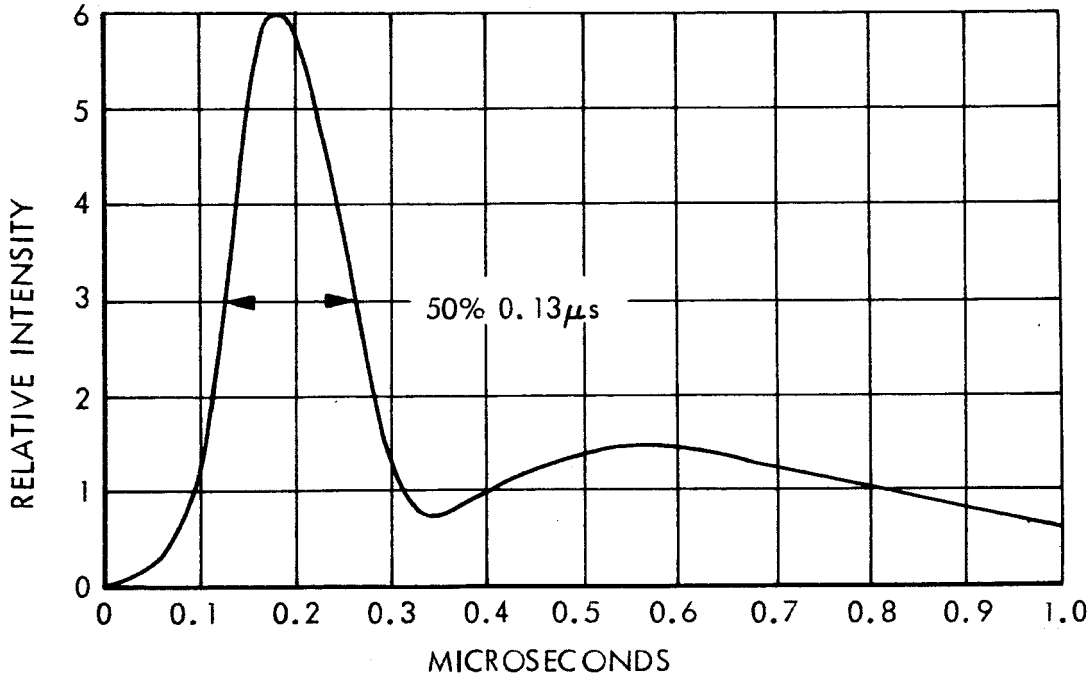

FIGURE 9 - U V PULSE SHAPE

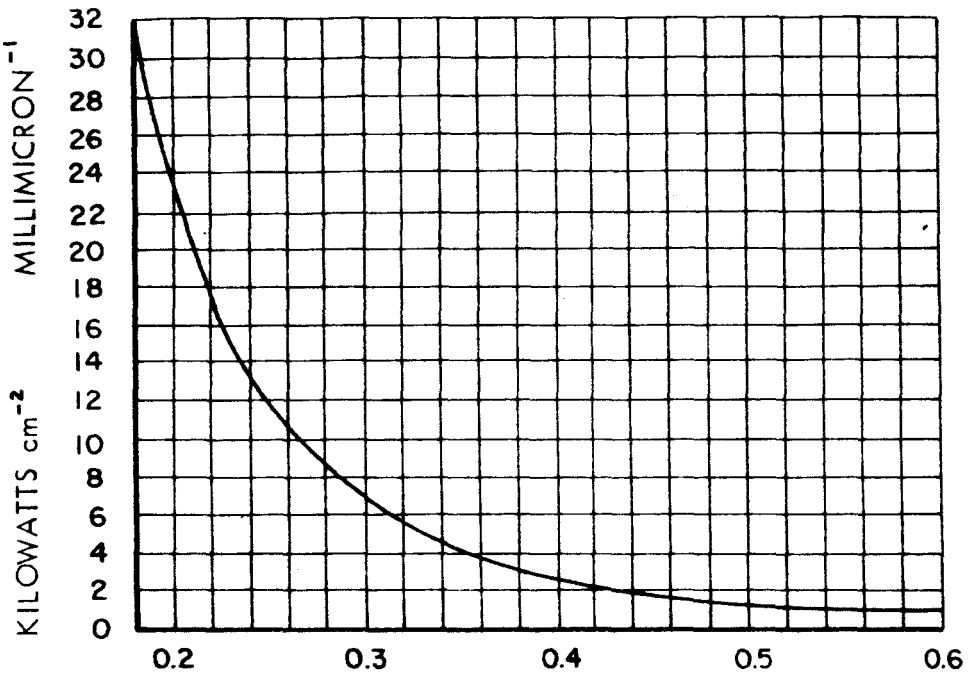

FIGURE 10 - 40,000°K BLACK BODY SPECTRAL DISTRIBUTION

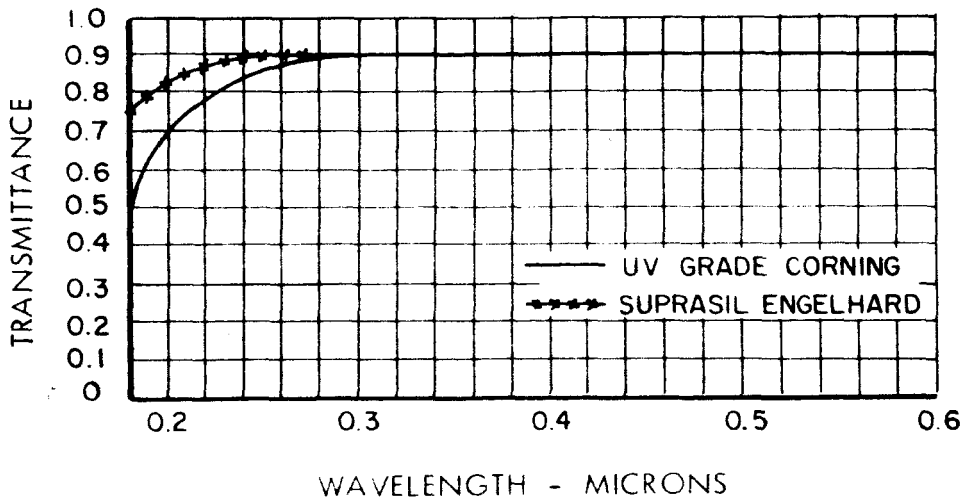

FIGURE 11 - TRANSMITTANCE 1cm FUSED SILICA

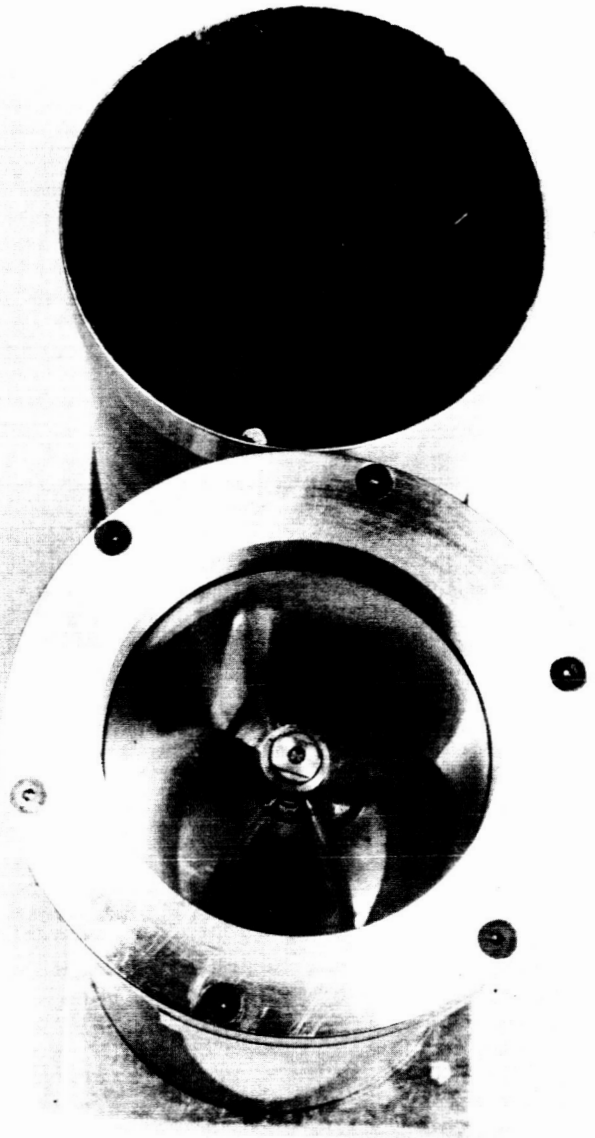

FIGURE 13 - TYPE 3, PARABOLIC UV TRANSMITTER

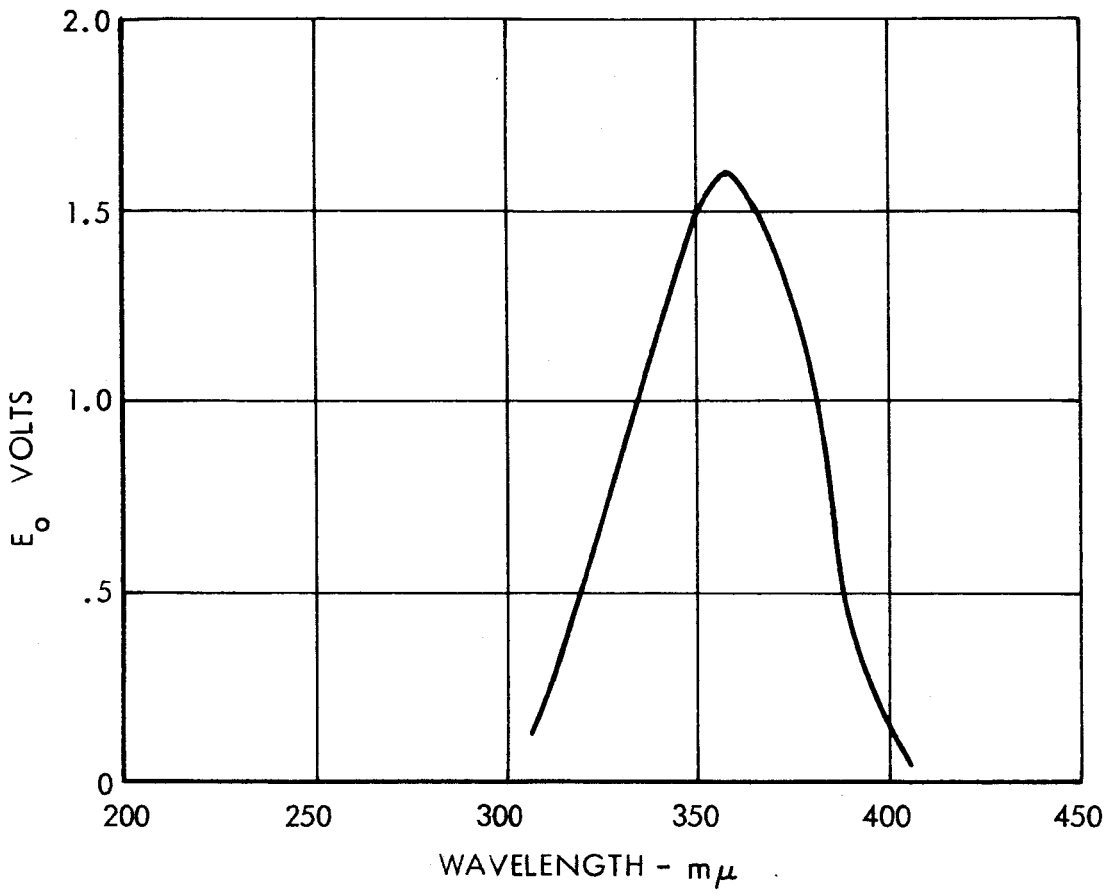

FIGURE 14 - UV PHOTOTRANSISTOR UNIT OUTPUT vs. WAVELENGTH

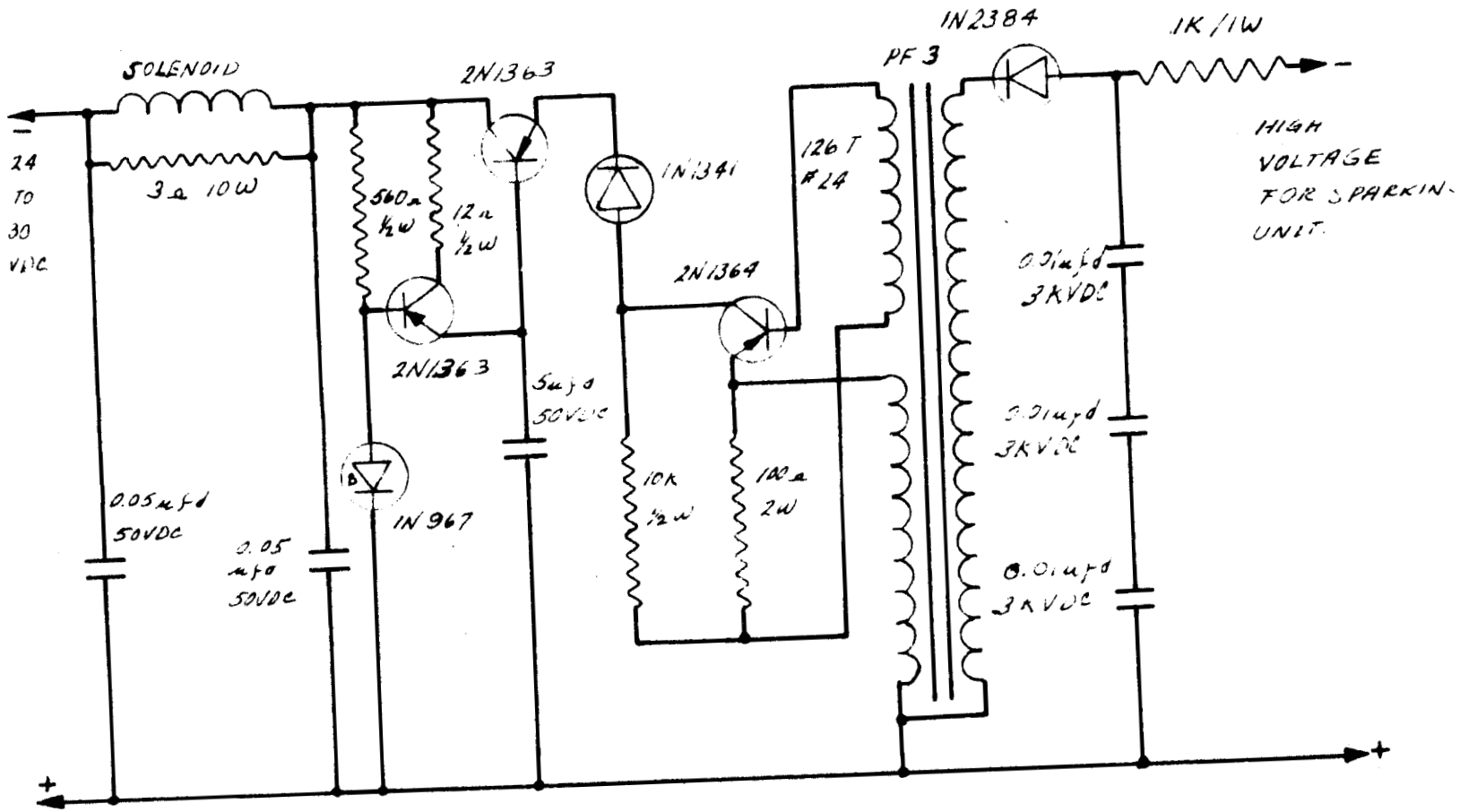

FIGURE 15 - SPARK HIGH VOLTAGE POWER SUPPLY

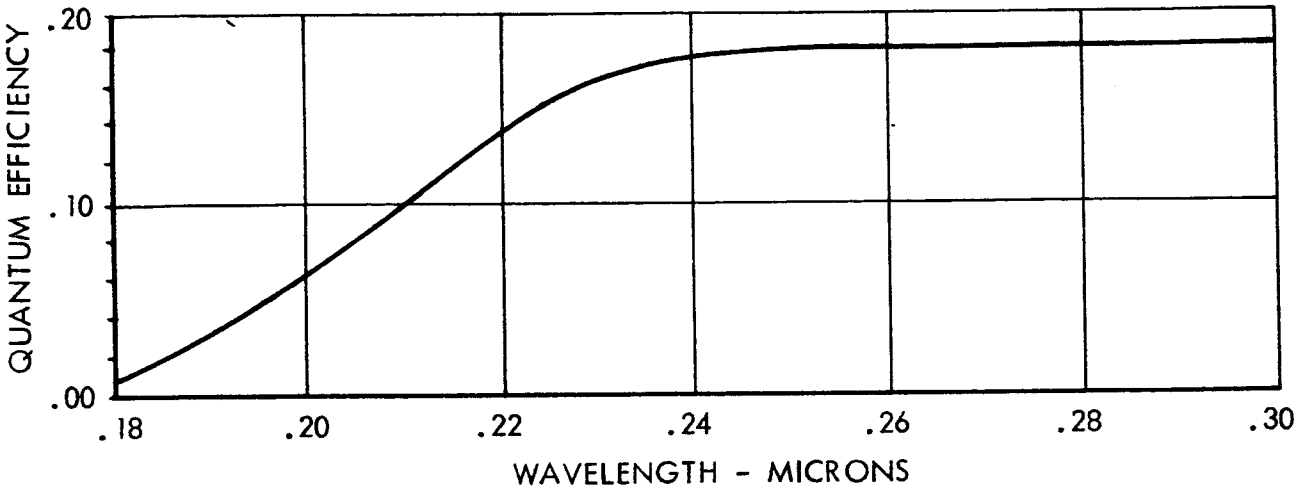

FIGURE 16 - QUANTUM EFFICIENCY 1P28

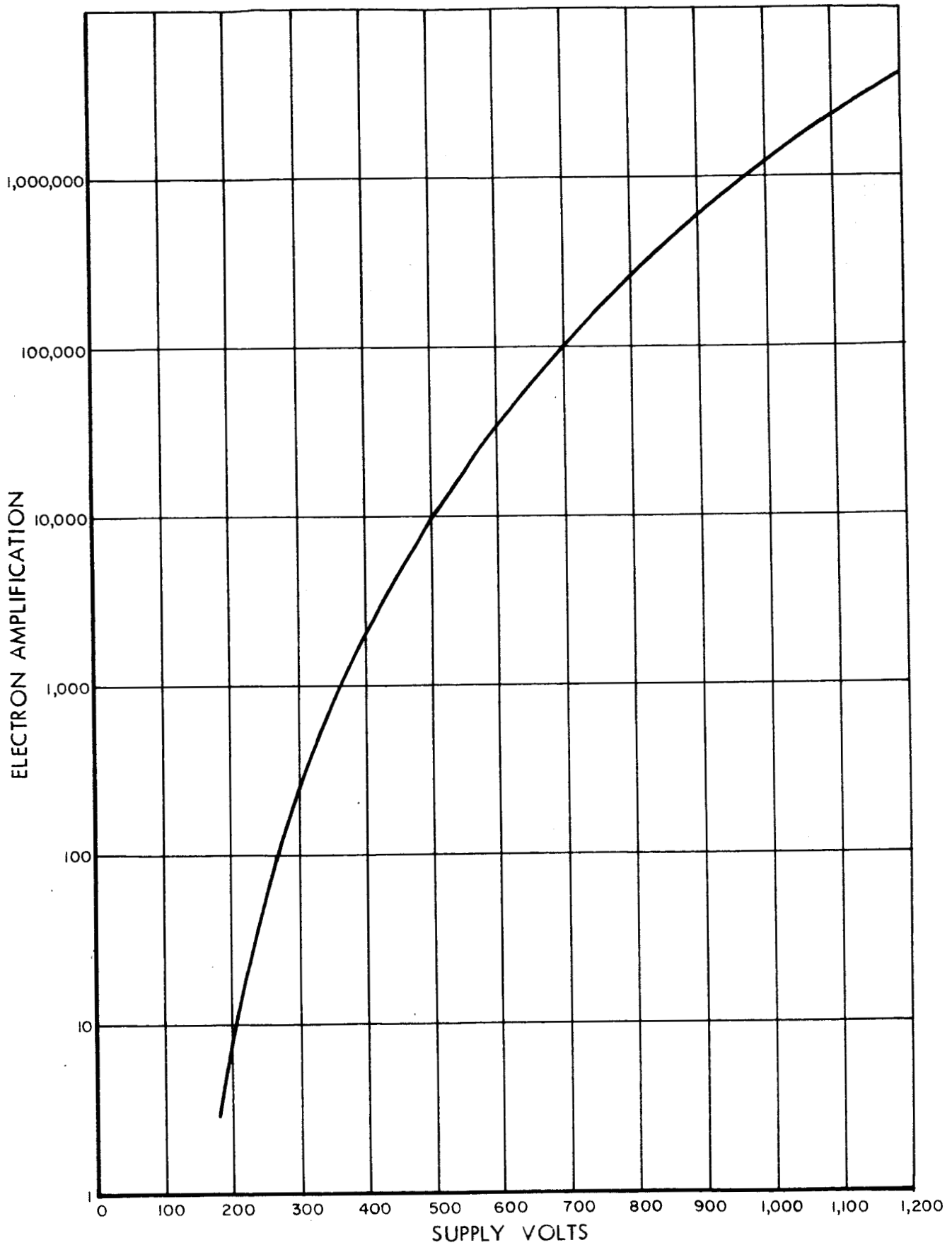

FIGURE 17 - RCA 1P28 ELECTRON AMPLIFICATION

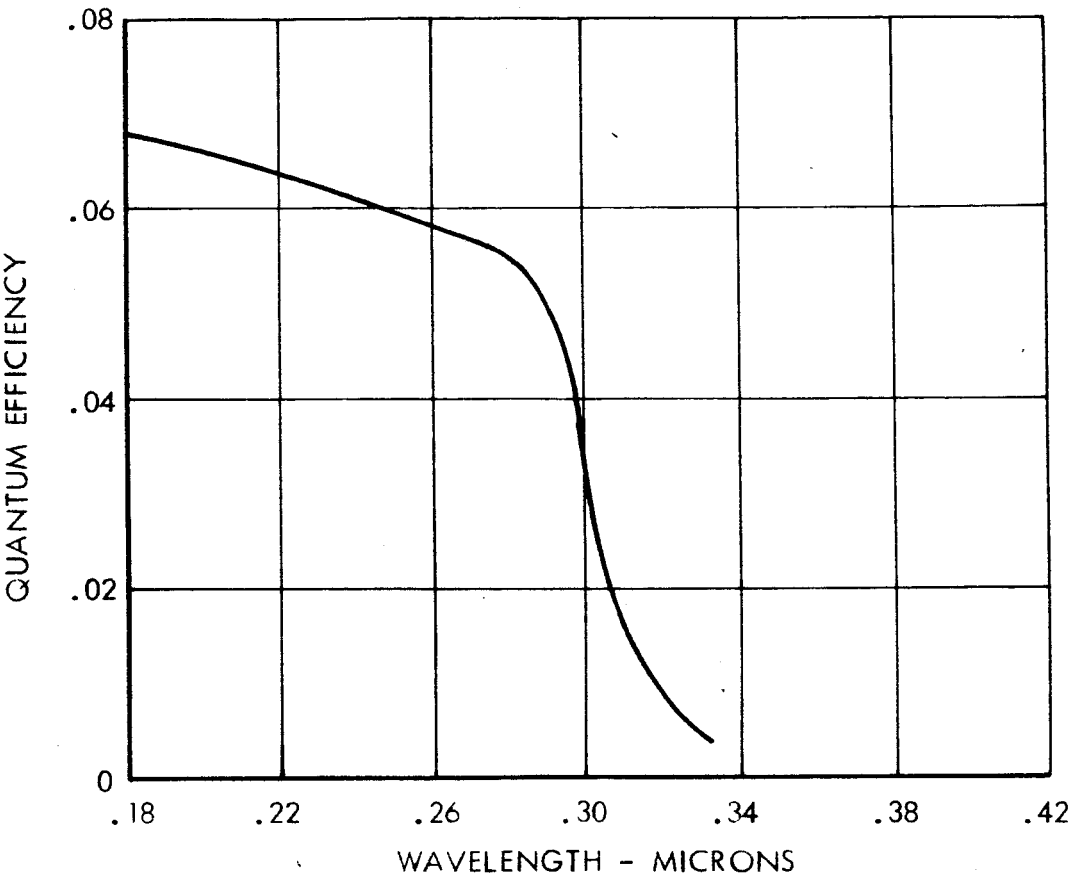

FIGURE 18 - C70127 (CsTe) QUANTUM EFFICIENCY vs. WAVELENGTH

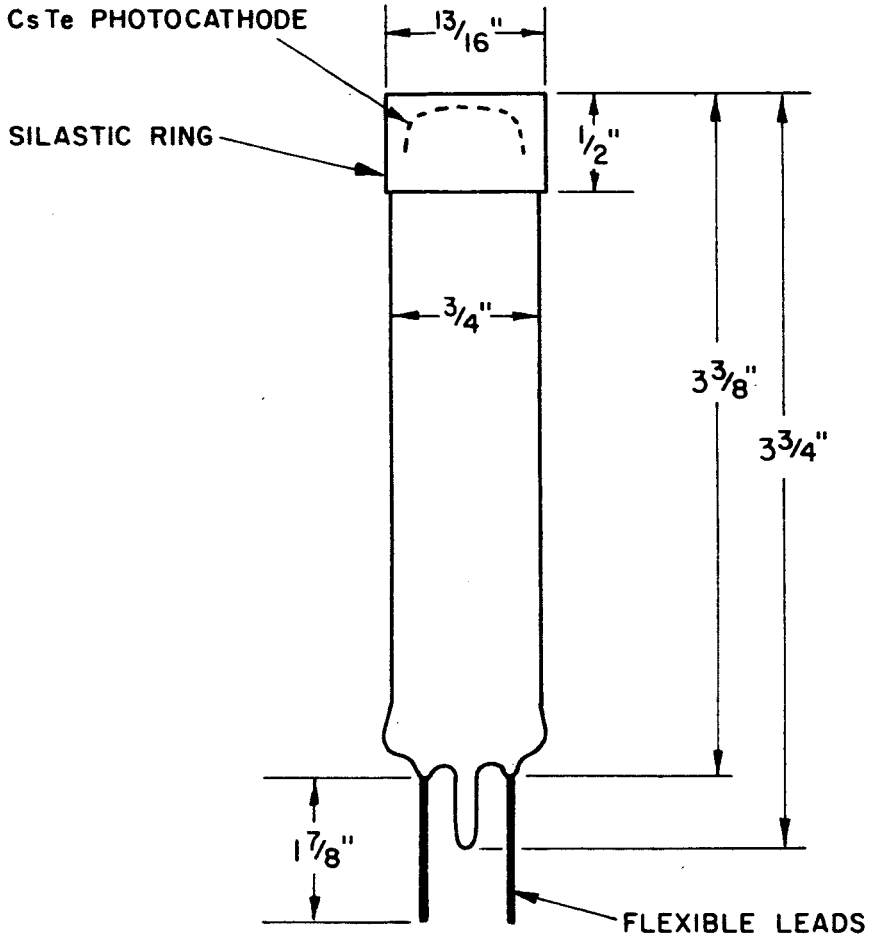

FIGURE 19 - C70127 OUTLINE DRAWING

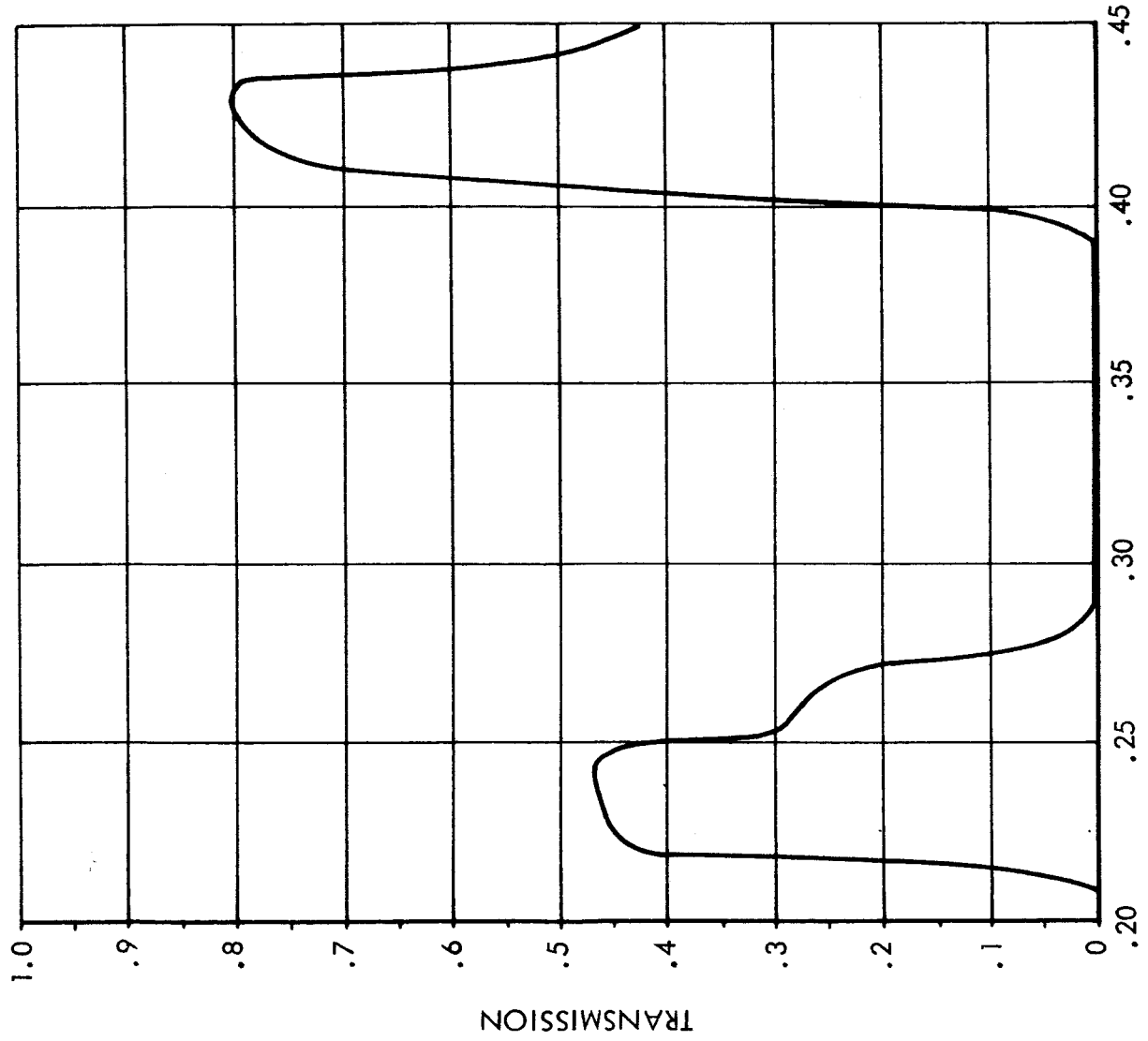

FIGURE 20 - TRANSMISSION 6 cm STP CHLORINE

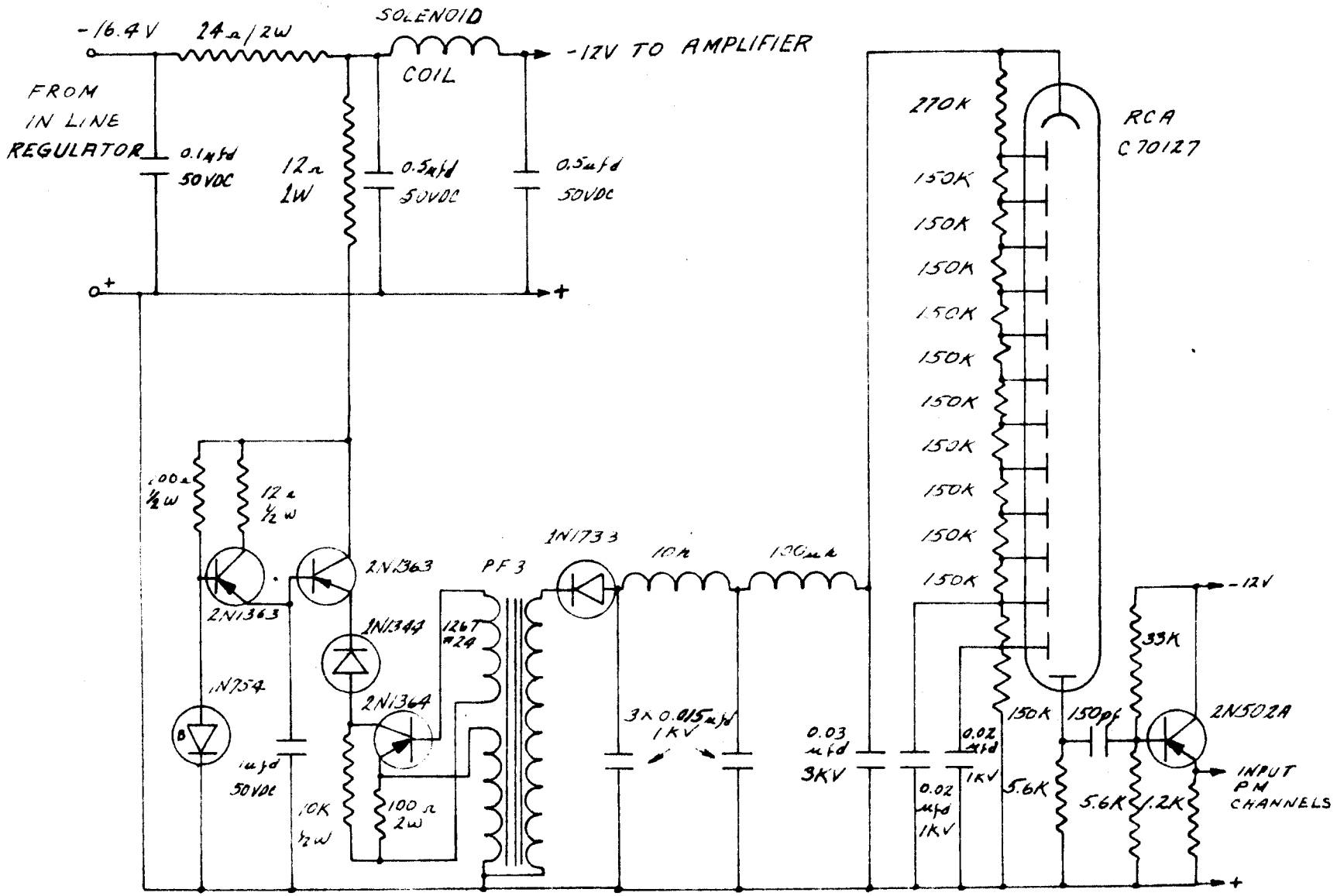

FIGURE 21 - RECEIVER PHOTOMULTIPLIER CIRCUIT

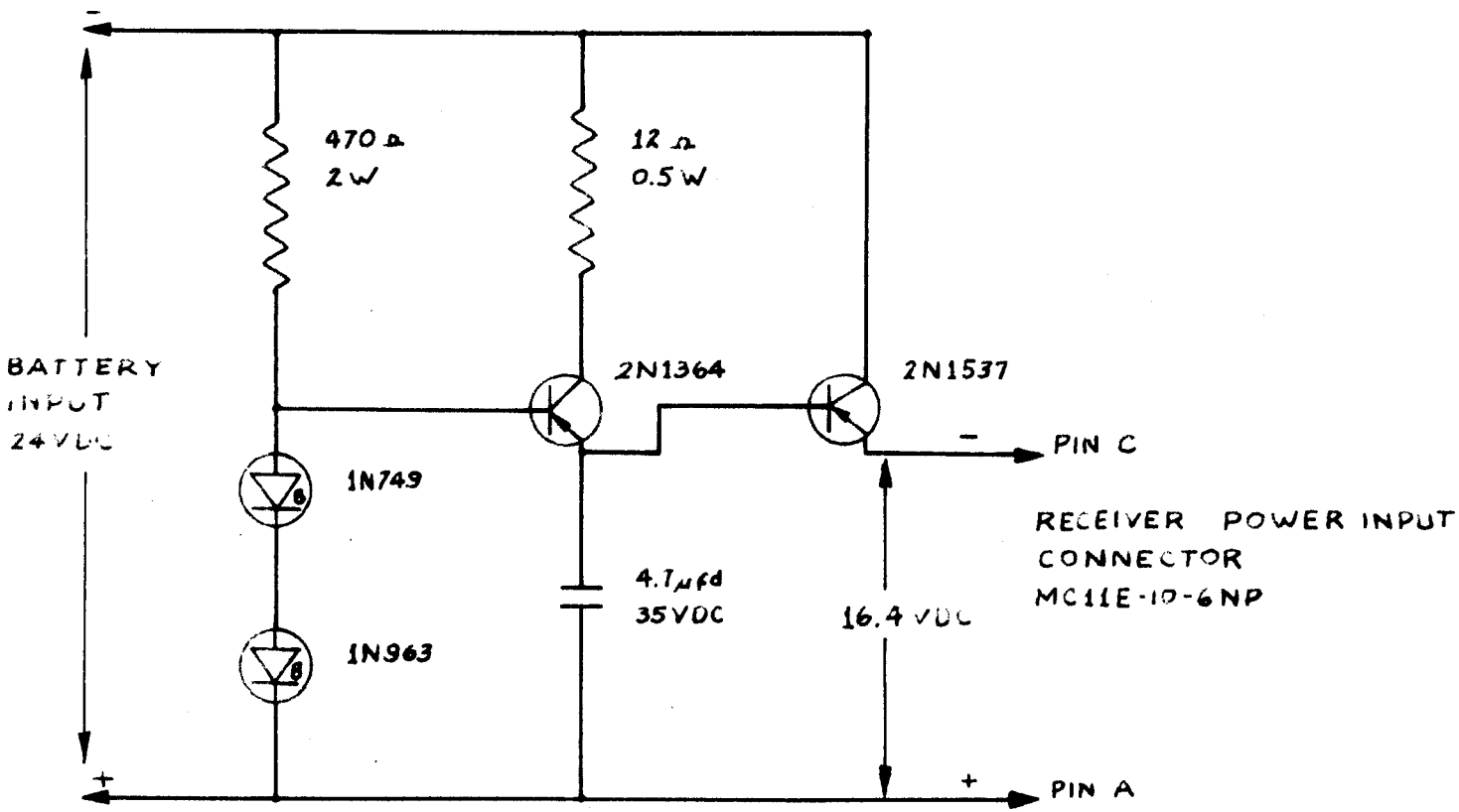

FIGURE 22 - RECEIVER VOLTAGE REGULATOR

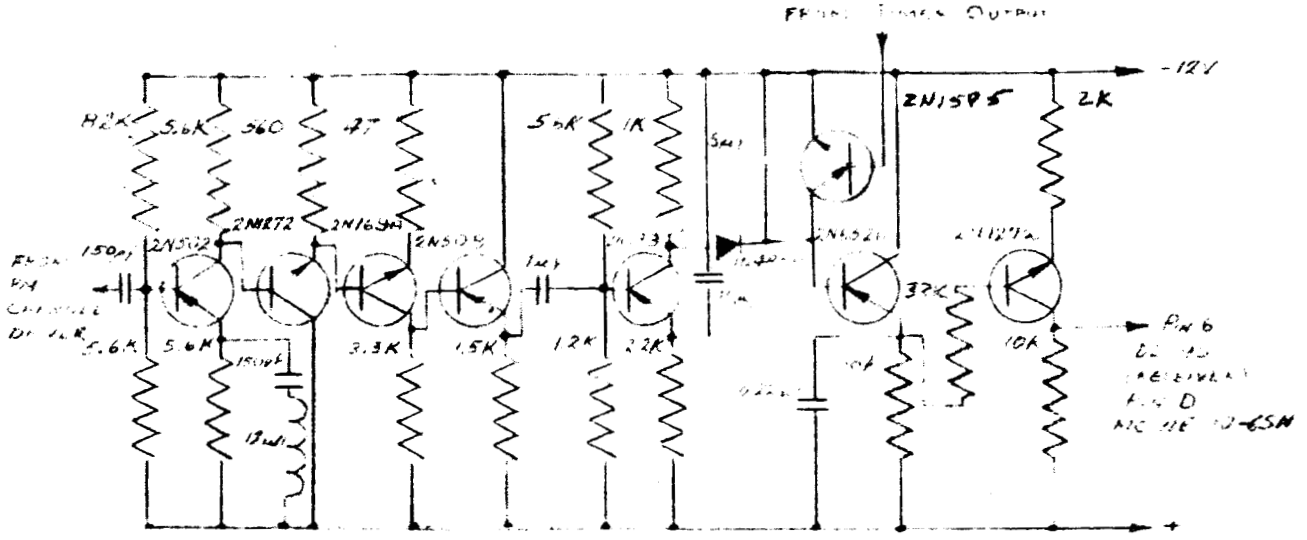

LOW SENSITIVITY AMPLIFIER - PM CHANNEL "D"

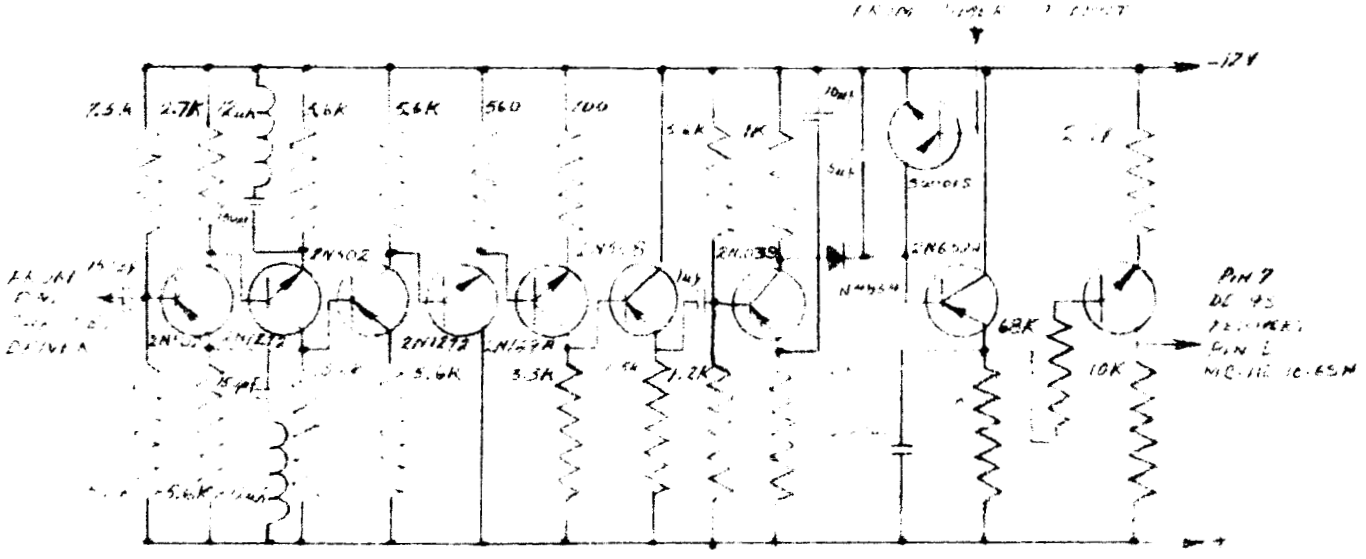

MEDIUM SENSITIVITY AMPLIFIER - PM CHANNEL "E"

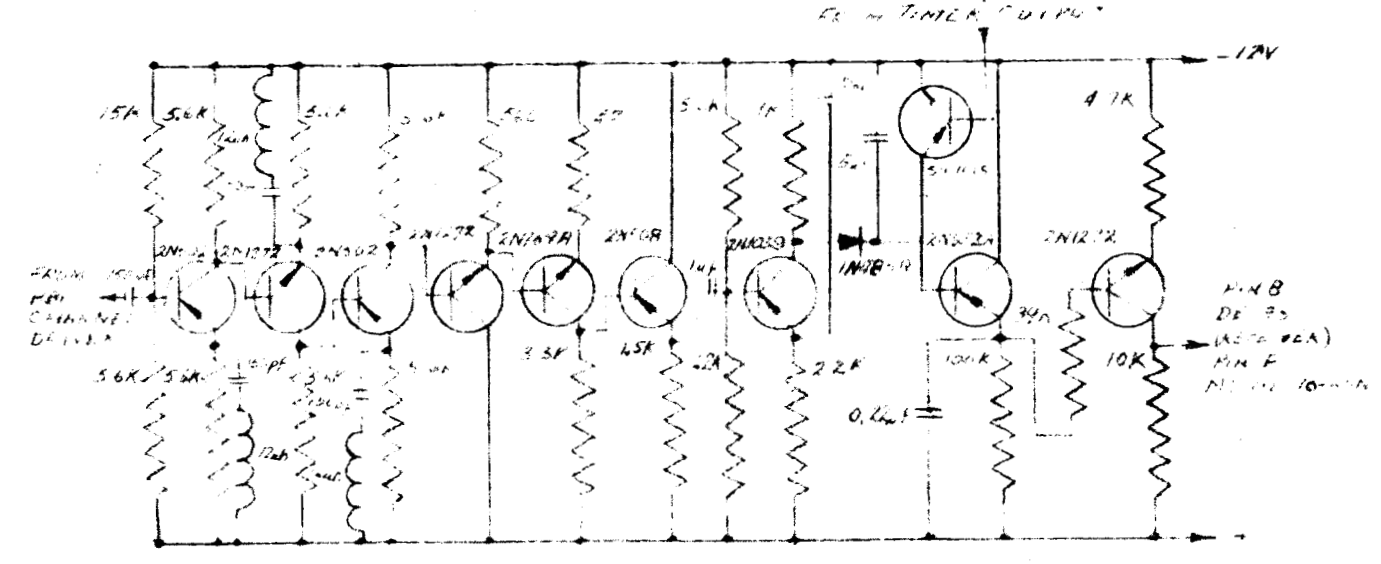

HIGH SENSITIVITY AMPLIFIER - PM CHANNEL "F"

FIGURE 23 - SCATTER PULSE AMPLIFIERS

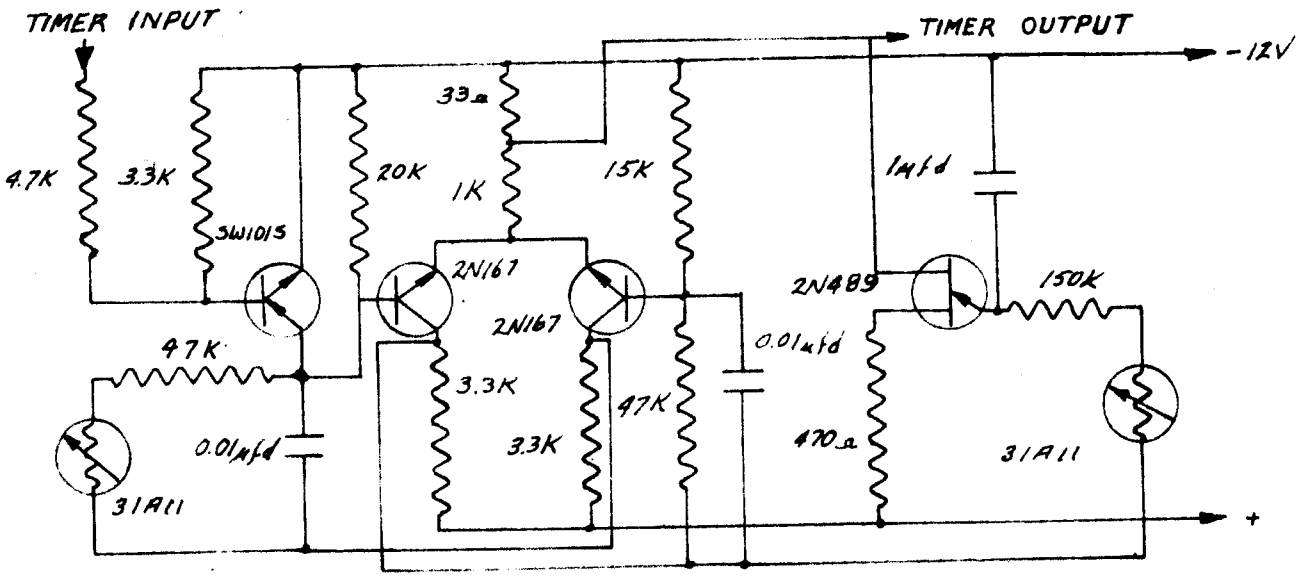

FIGURE 24 - TIMING CIRCUIT

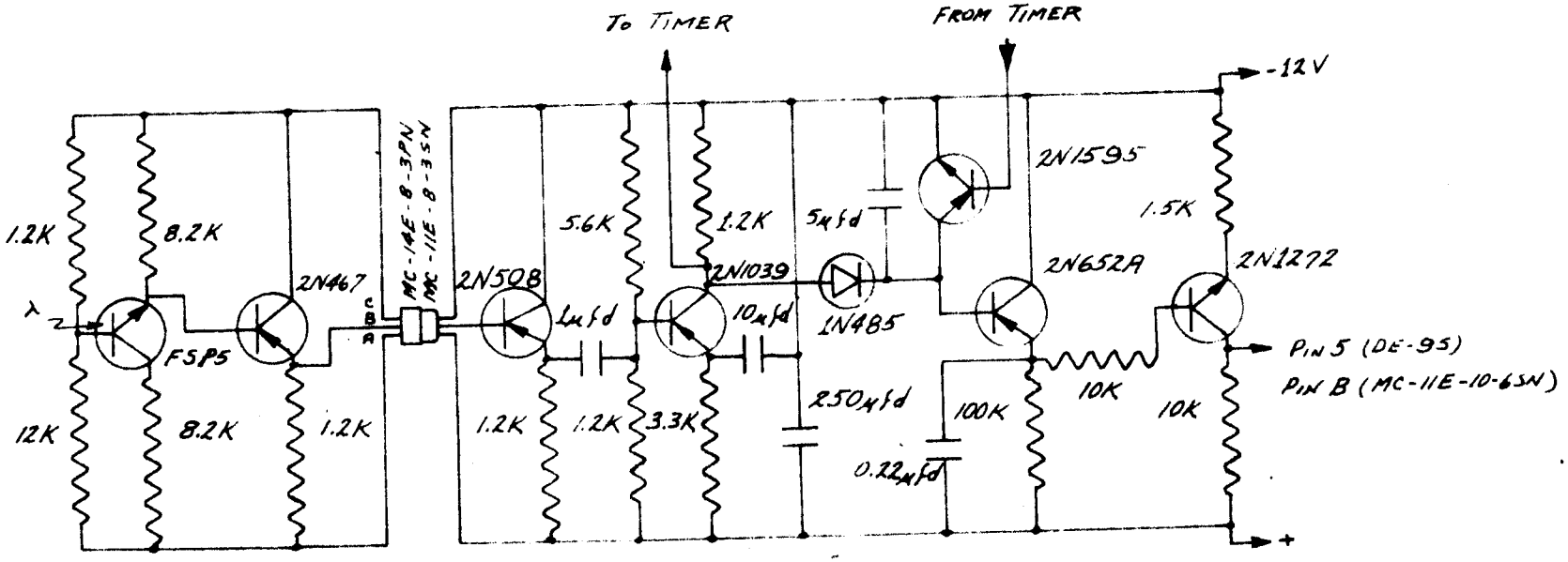

FIGURE 25 - PHOTOTRANSISTOR AMPLIFIER

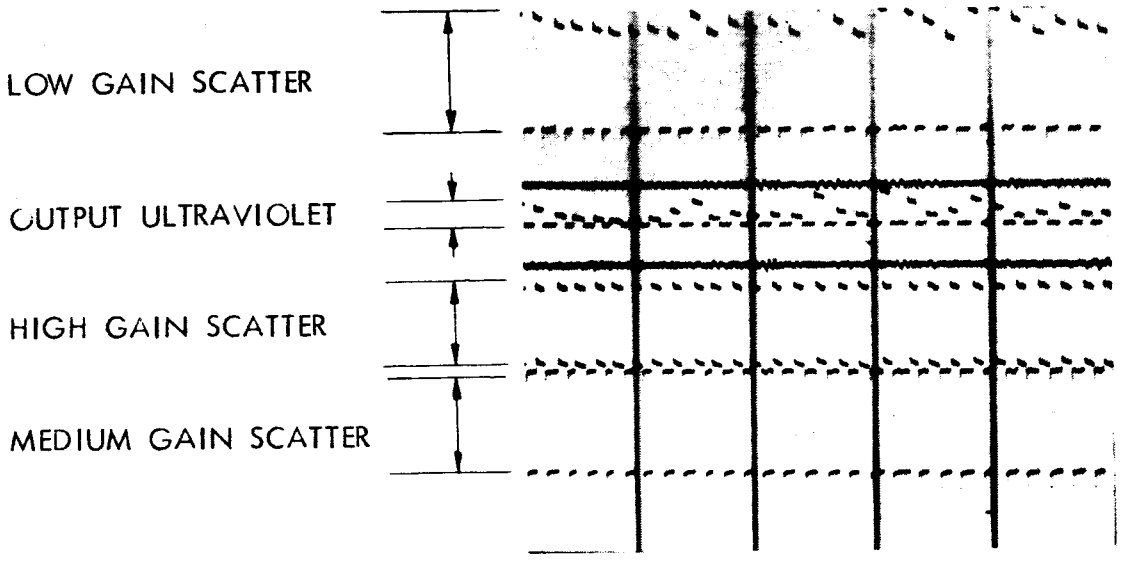

ALTITUDE 800 METERS
AIR DENSITY 1.175 Kg m^{-3}

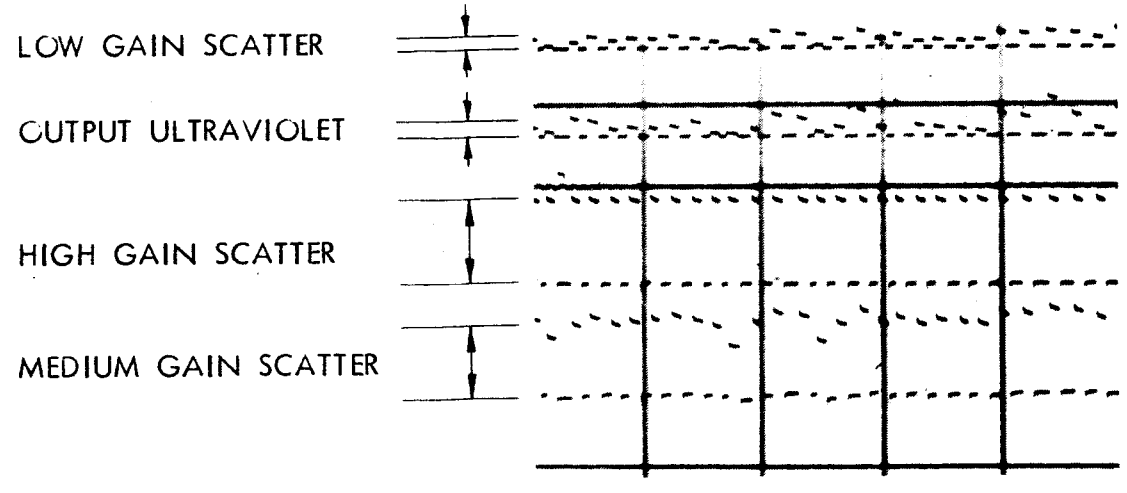

ALTITUDE 9700 METERS
AIR DENSITY .450 Kg m^{-3}

FIGURE 26 - FLIGHT DATA - F-104 FLIGHT

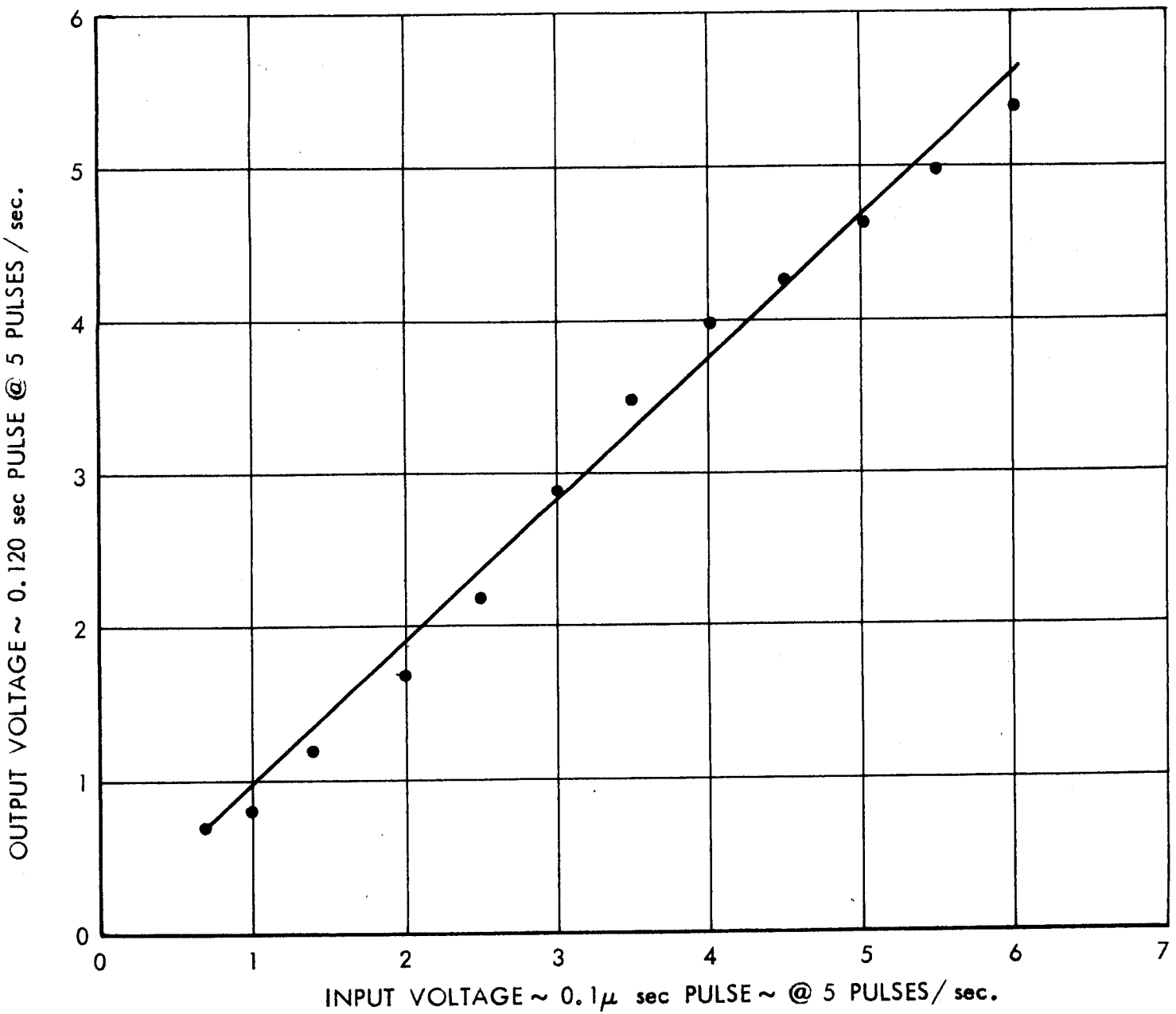

FIGURE 27 - PULSE AMPLIFIER RESPONSE CHARACTERISTICS

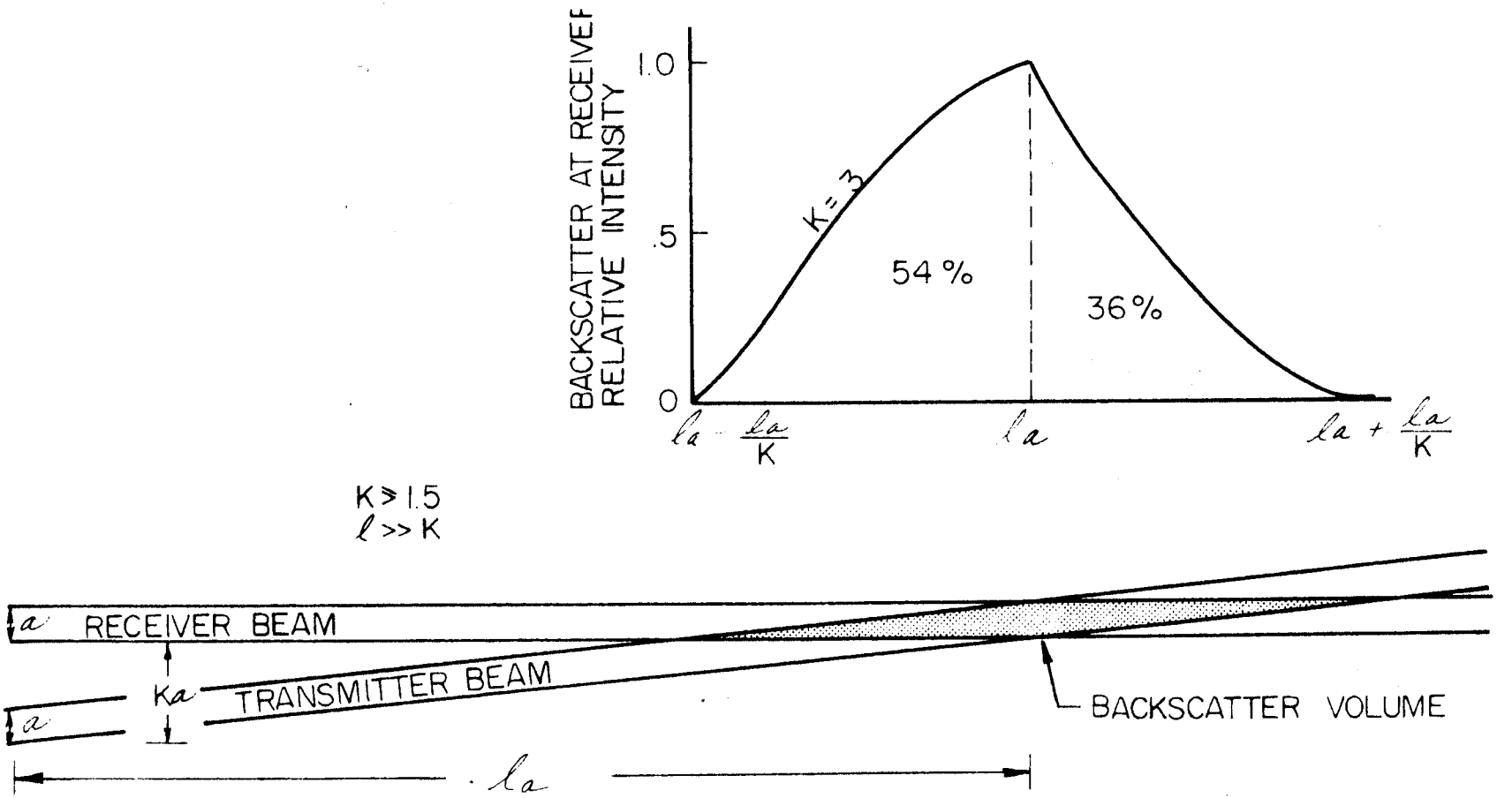

FIGURE 28 - BACKSCATTER GEOMETRY

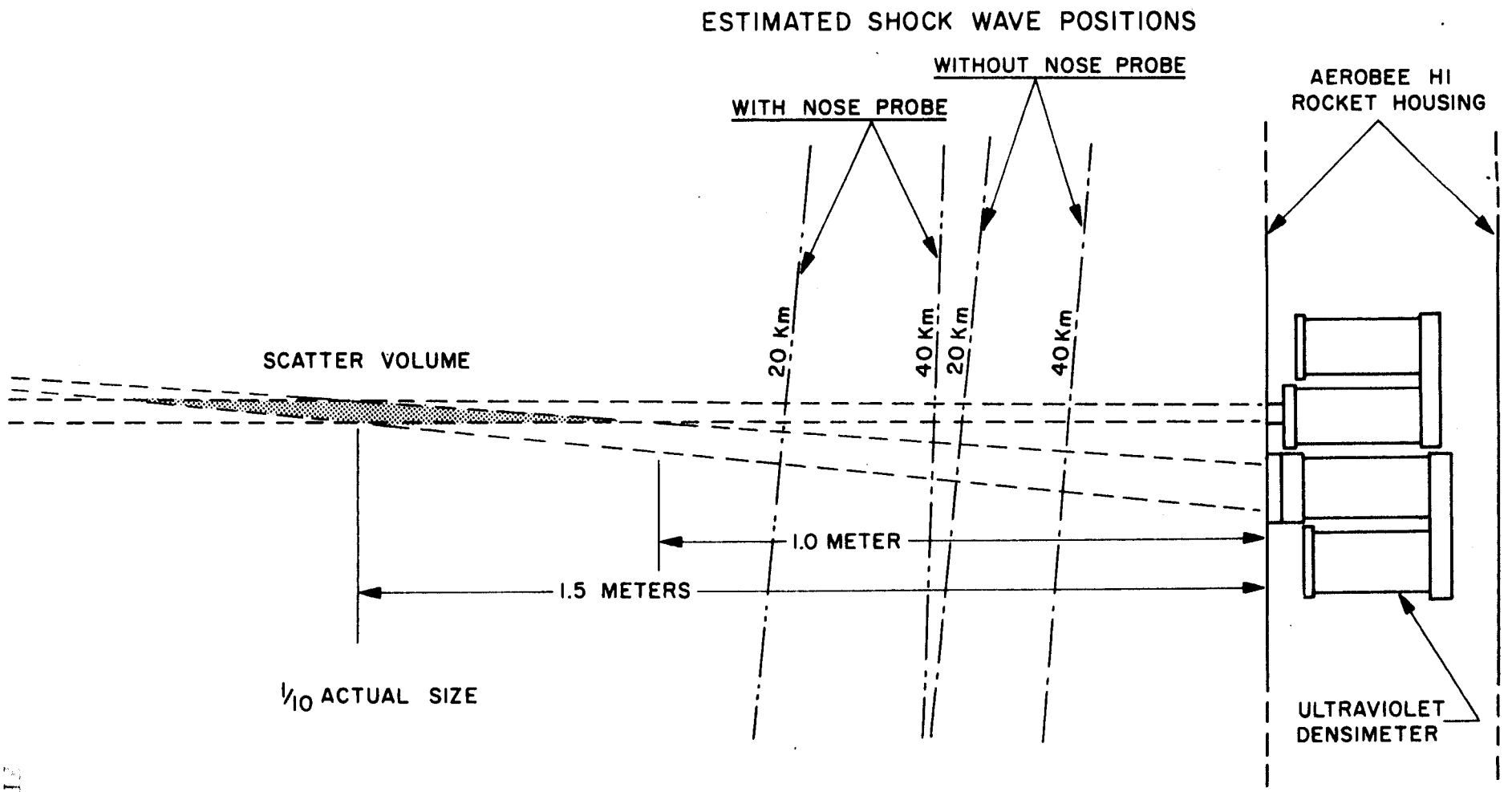

FIGURE 29 - AEROBEE BACKSCATTER GEOMETRY

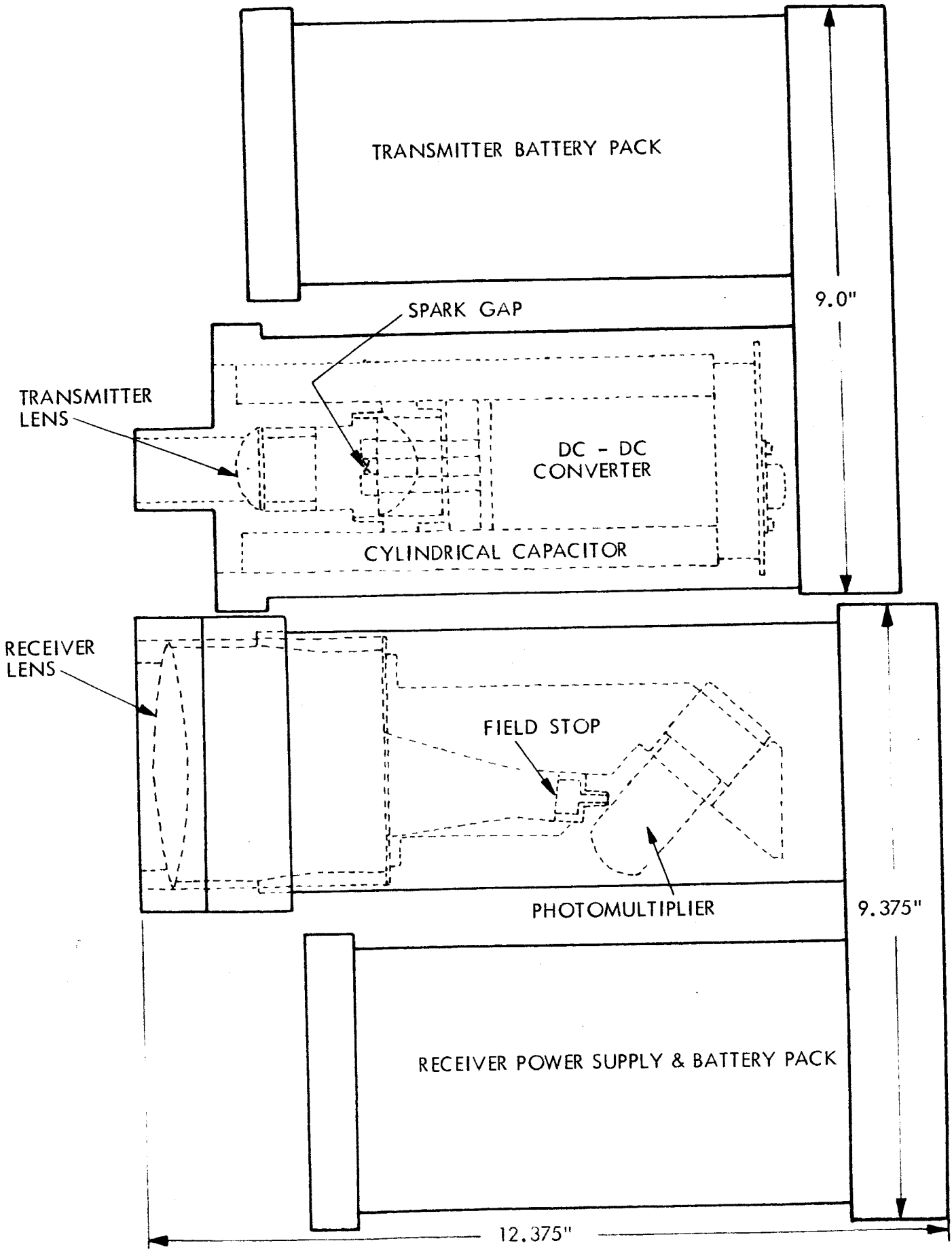

FIGURE 30 - TYPE 2 ULTRAVIOLET DENSIMETER

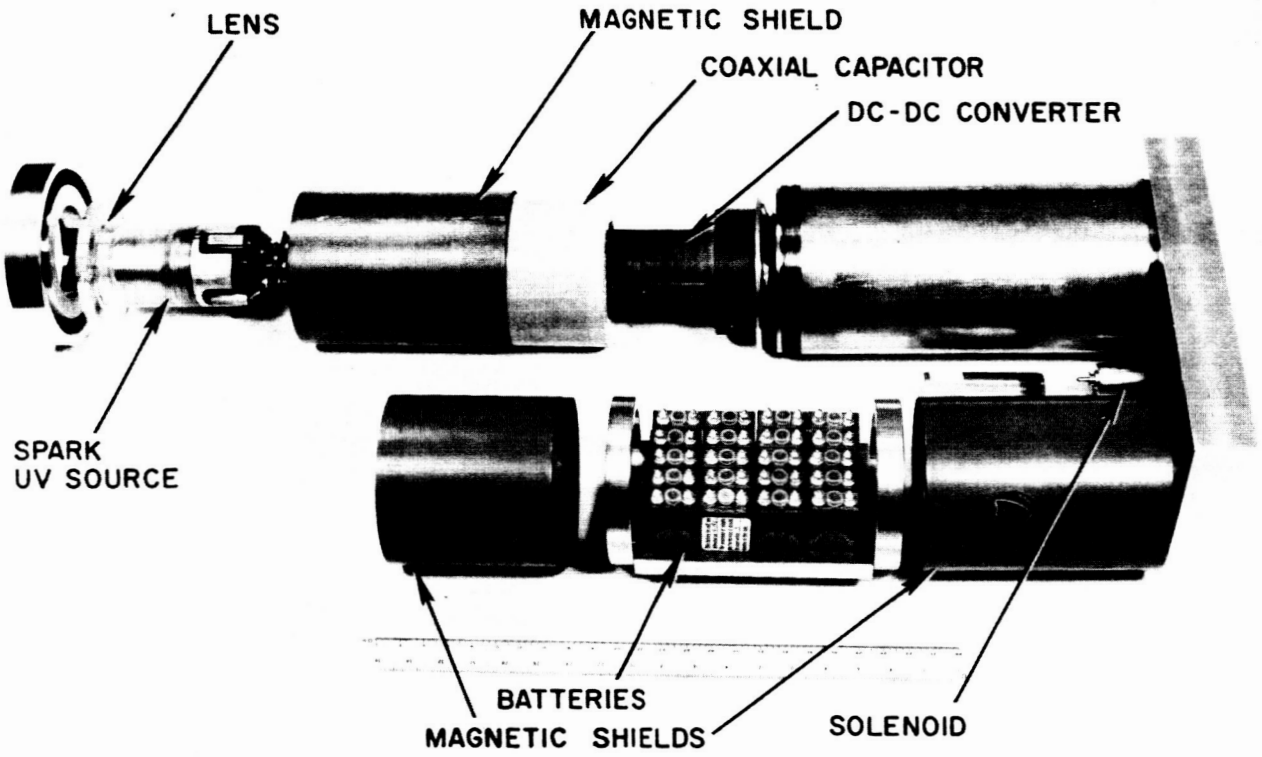

FIGURE 31 - COMPONENTS TYPE 2 UV TRANSMITTER

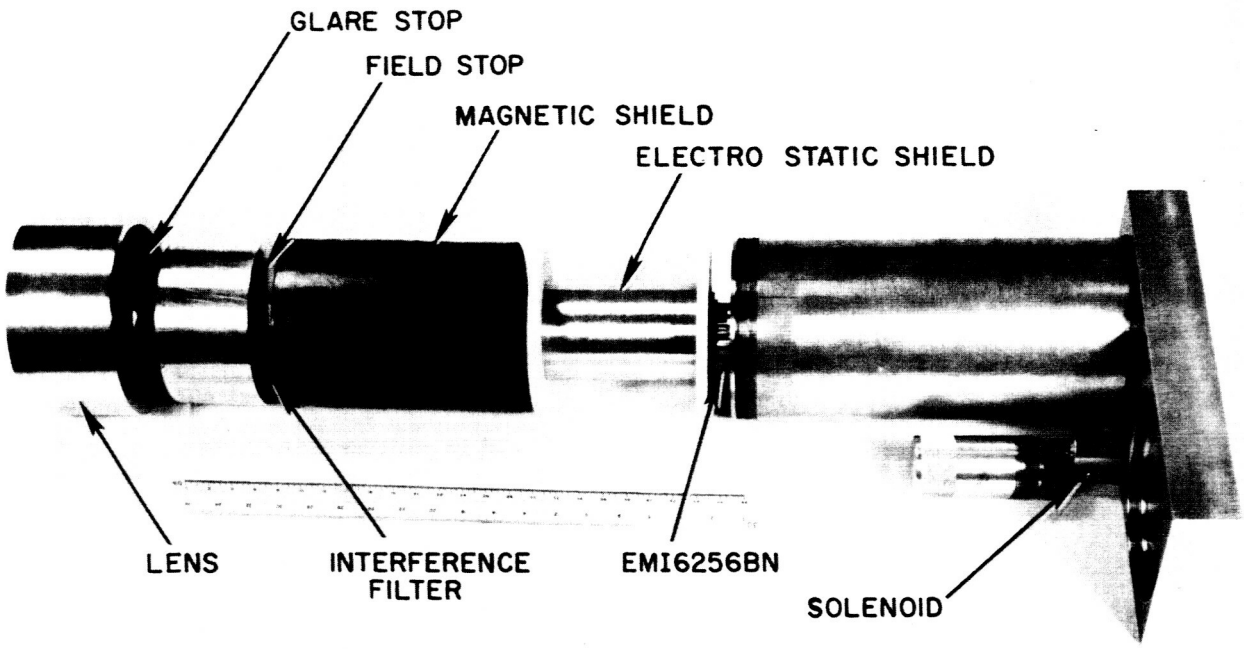

FIGURE 33 - COMPONENTS UV RECEIVER

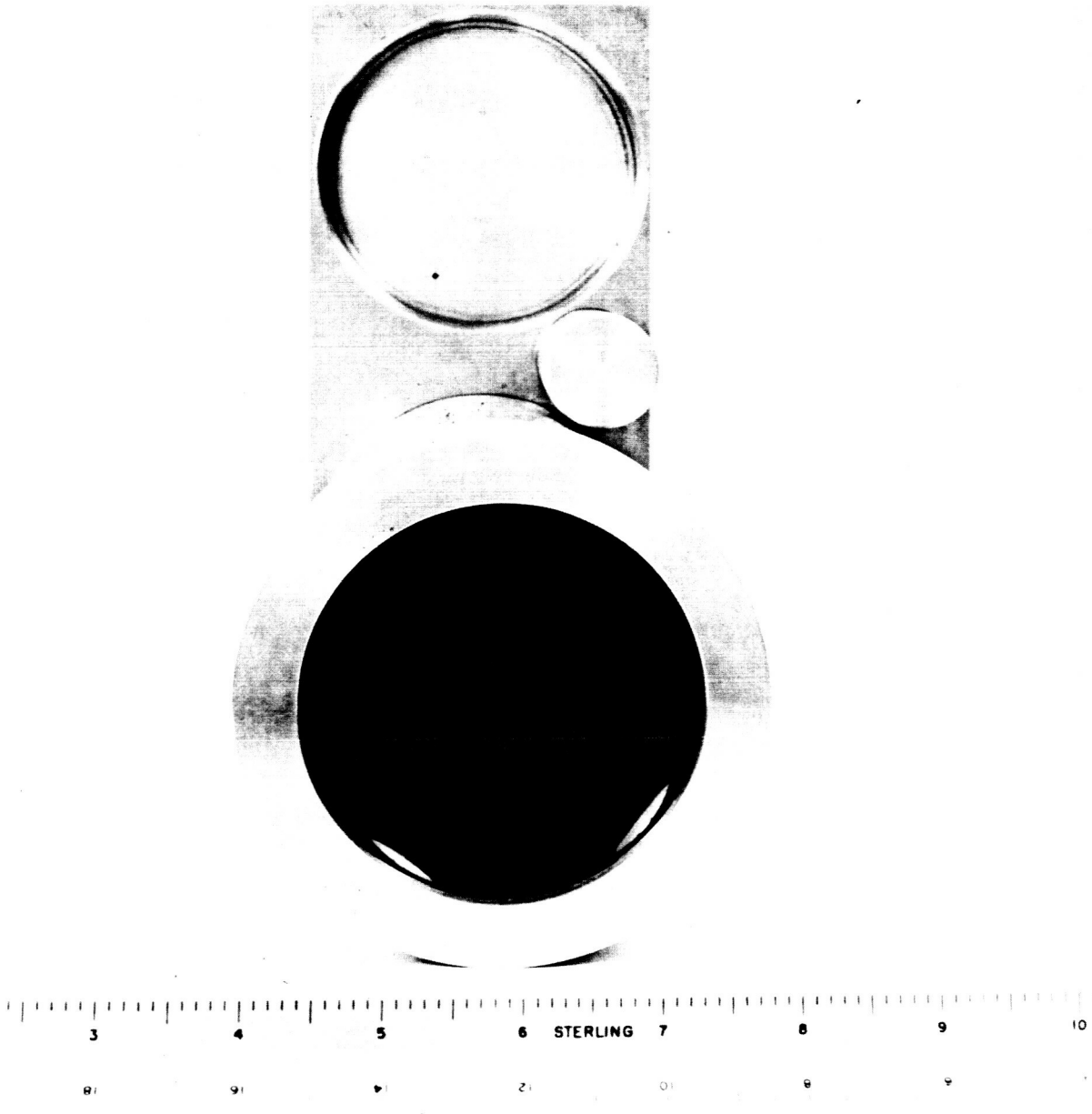

FIGURE 34 - FRONT UV RECEIVER

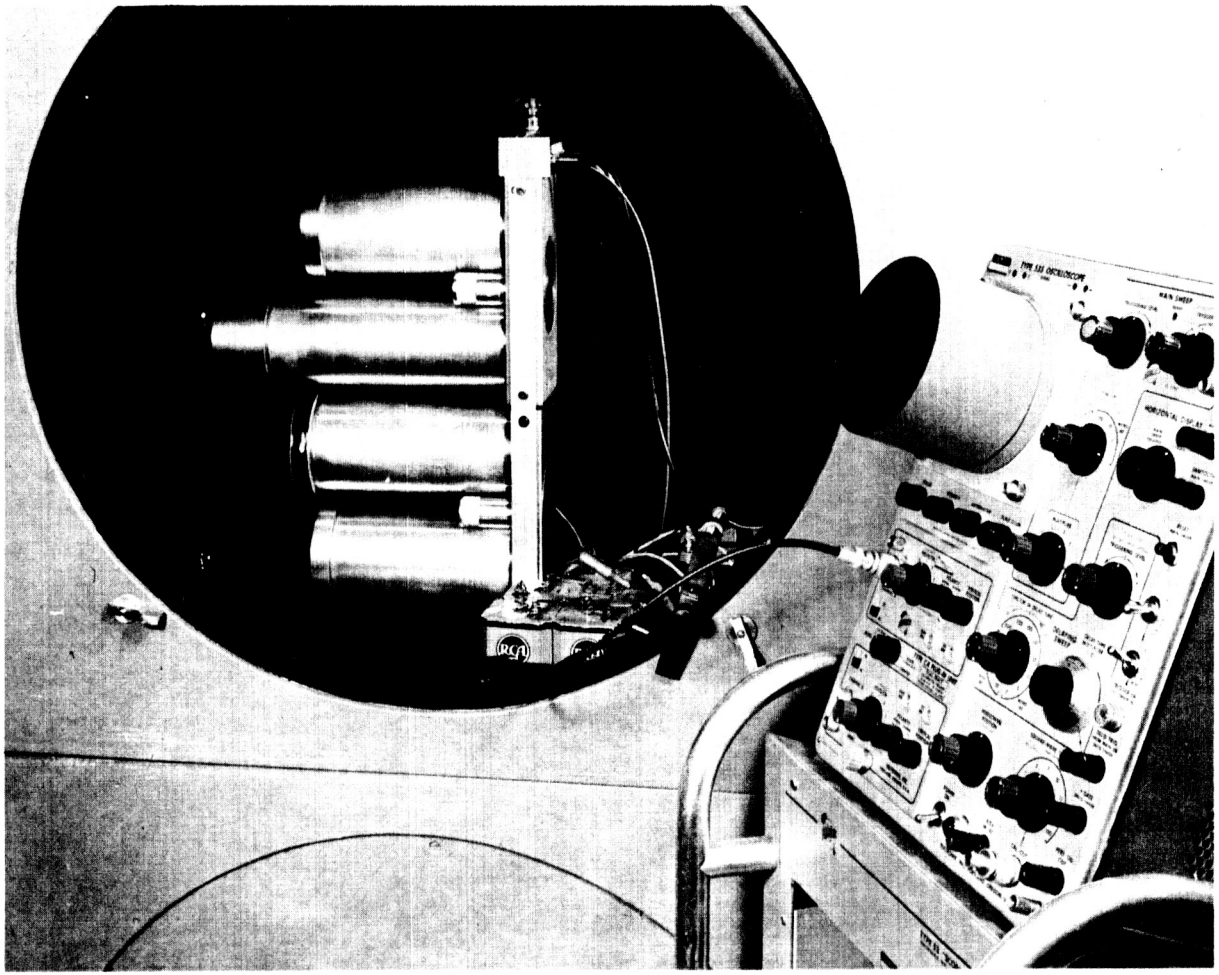

FIGURE 35 - SIDE VIEW OF UV DENSIMETER

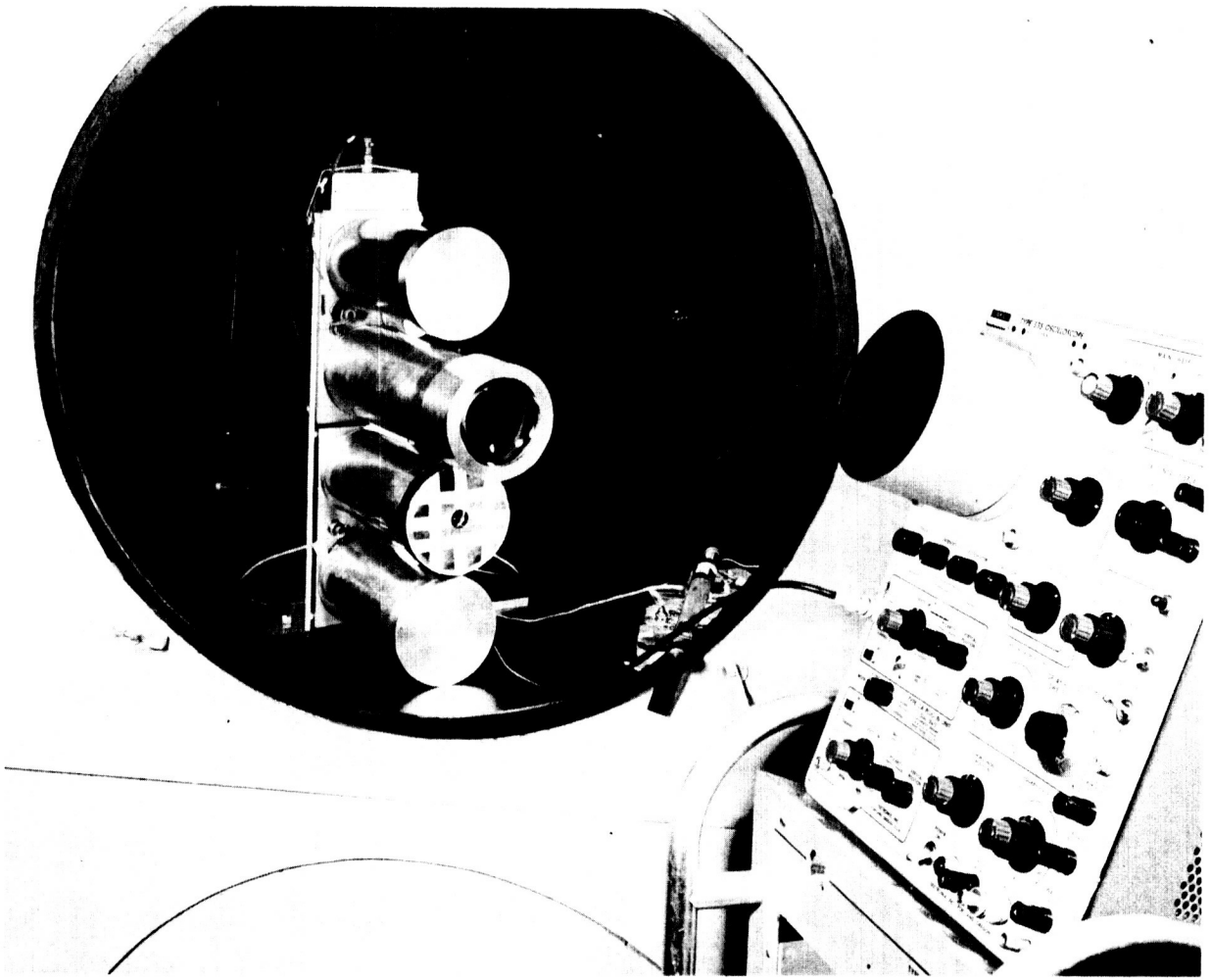

FIGURE 36 - FRONT VIEW OF UV DENSIMETER

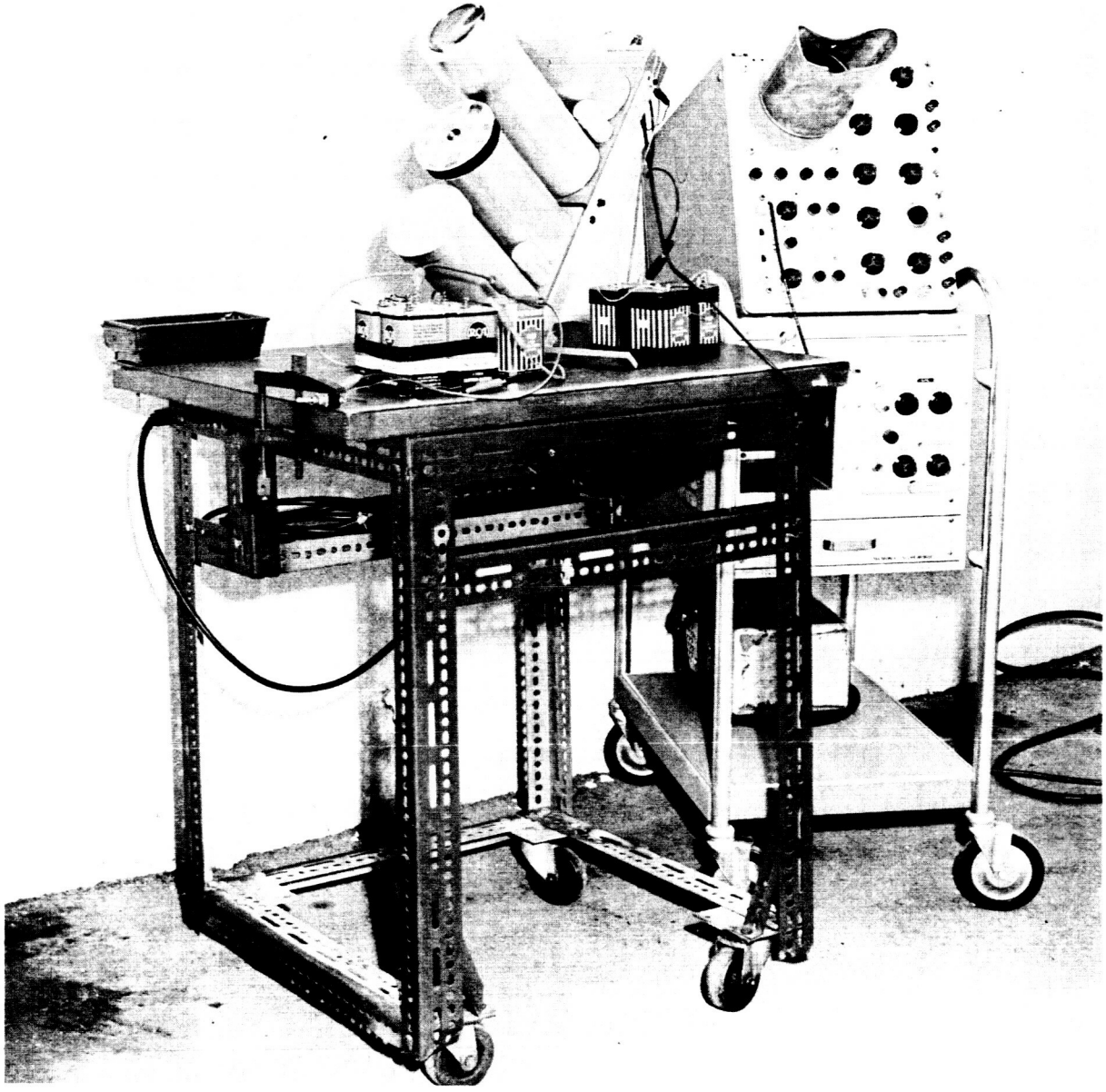

FIGURE 37 - UV DENSIMETER IN OUTSIDE DAYLIGHT TEST

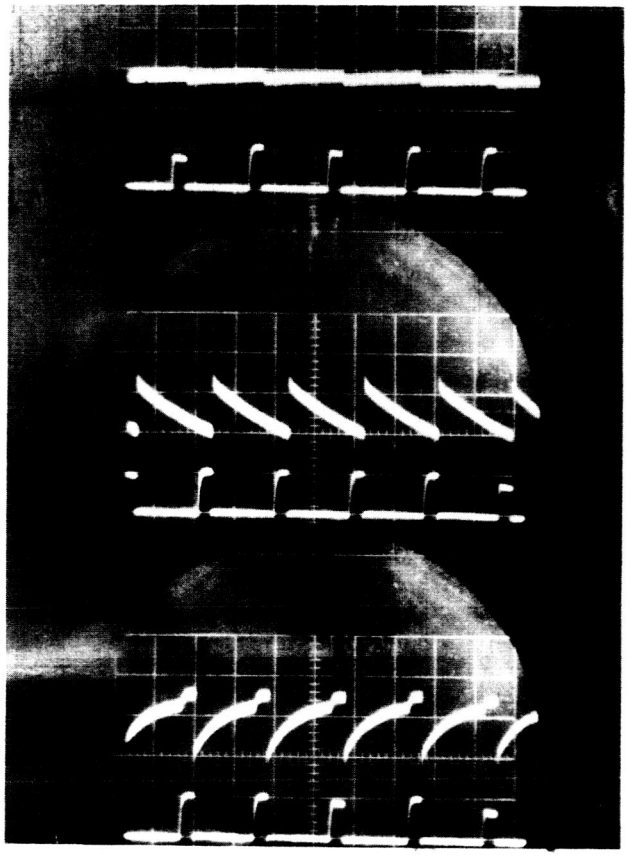

0.050 V / div. LOW GAIN

5 V / div. UV PULSE

0.050 V / div. MEDIUM GAIN

5 V / div. UV PULSE

0.050 V / div. HIGH GAIN

5 V / div. UV PULSE
TIME 0.2 sec/div.

FIGURE 38 - COVERED RECEIVER LENS SIGNAL OUTPUT

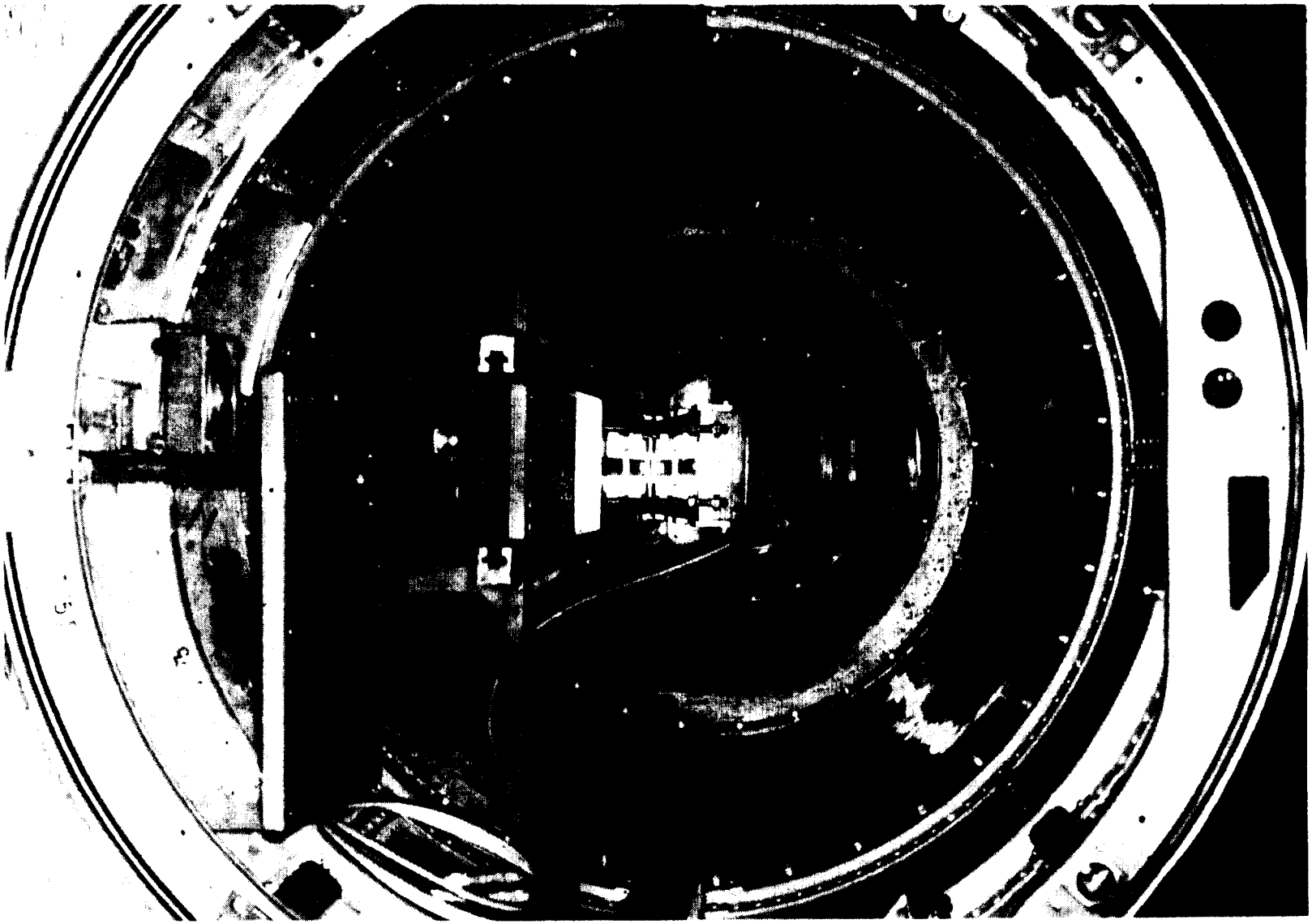

FIGURE 40 - INTERNAL VIEW F-104 NOSE - NASA PHOTO E-9221

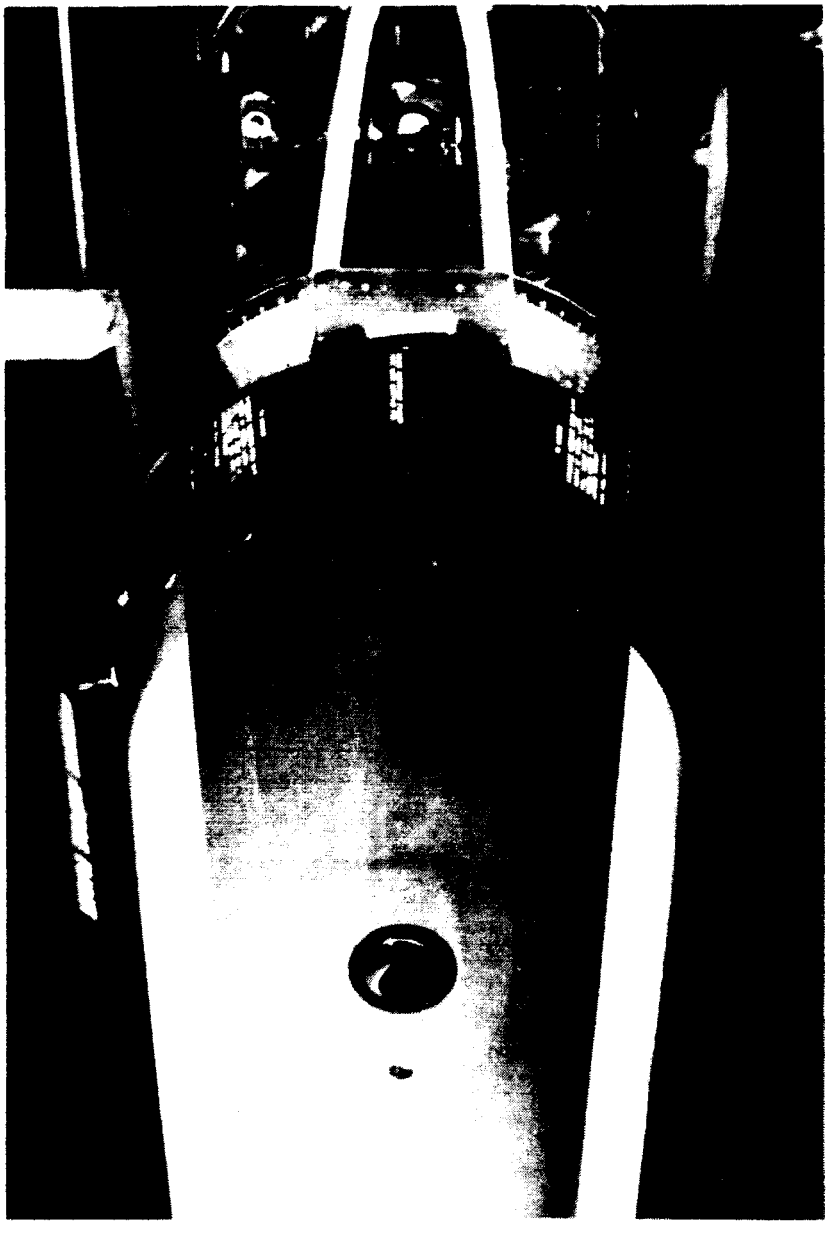

FIGURE 41 - EXTERNAL VIEW F-104 NOSE

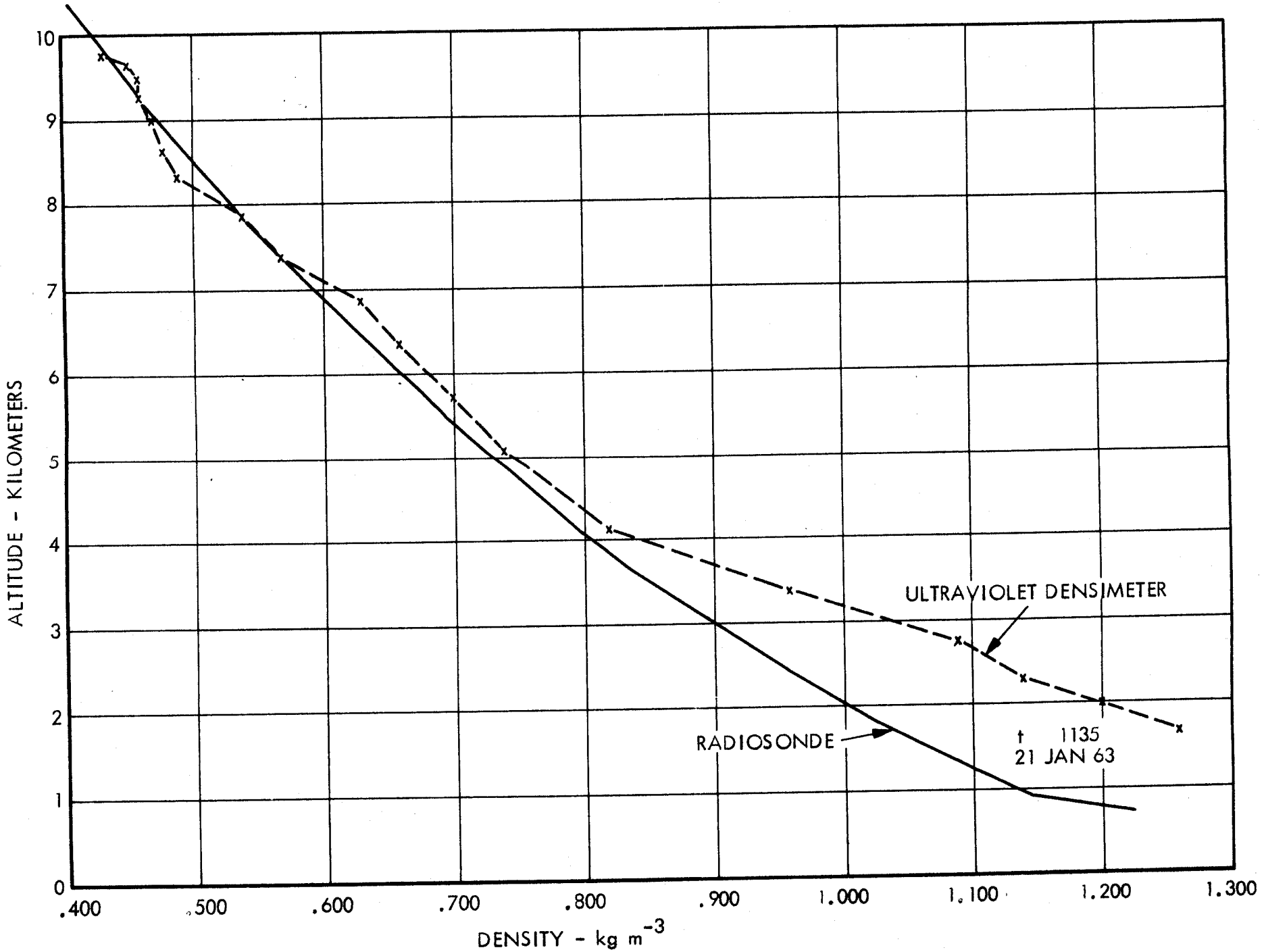

FIGURE 42 - ULTRAVIOLET DENSIMETER DATA vs. RADIOSONDE